A methodological framework of travel time distribution estimation for urban signalized arterial roads

Zheng, Fangfang; Van Zuylen, Henk; Liu, Xiaobo

DOI
10.1287/trsc.2016.0718

Publication date
2017

Document Version
Accepted author manuscript

Published in
Transportation Science

Citation (APA)
Zheng, F., Van Zuylen, H., & Liu, X. (2017). A methodological framework of travel time distribution estimation for urban signalized arterial roads. *Transportation Science*, *51*(3), 893-917. https://doi.org/10.1287/trsc.2016.0718

A methodological framework of travel time distribution estimation for urban signalized arterial roads

Fangfang Zheng [1,2], Xiaobo Liu[1,2], Henk van Zuylen[1,3]

[1] School of Transportation and Logistics, Southwest Jiaotong University, No. 111 Erhuanlu Beiyiduan, 610031, Chengdu, P.R. China

[2] National-Local Association Laboratory of Comprehensive Transportation Intelligentization, Southwest Jiaotong University, No. 111 Erhuanlu Beiyiduan, 610031, Chengdu, P.R. China

[3] Department of Transport and Planning, Delft University of Technology, Stevinweg 1, 2628CN, Delft, the Netherlands

Abstract

Urban travel times are rather variable due to a lot of stochastic factors both in traffic flows, signals and other conditions on the infrastructure. However, the most common way both in literature and practice is to estimate or predict only expected travel times, not travel time distributions. By doing so, it fails to provide full insight into the travel time dynamics and variability on urban roads. Another limitation of this common approach is that the effect of traffic measures on travel time reliability cannot be evaluated.

In this paper, an analytical travel time distribution model is presented especially for urban roads with fixed-time controlled intersections by investigating the underlining mechanisms of urban travel times. Different from mean travel time models or deterministic travel time models, the proposed model takes stochastic properties of traffic flow, stochastic arrivals and departures at intersections and traffic signal coordination between adjacent intersections into account, and therefore, is able to capture the delay dynamics and uncertainty at intersections. The proposed model was further validated with

both VISSIM simulation data and field GPS data collected in a Chinese city. The results demonstrate that the travel time distributions derived from the analytical model can well represent those from VISSIM simulation. The comparison with field GPS data shows that the model estimated link travel time distributions can also represent the field travel time distributions, though a small discrepancy can be observed in middle range travel times and higher travel times. We expect that the proposed model can be applied to influence travel time variability on signalized roads in terms of e.g. signal optimization.

Keywords: travel time distribution; simulation; urban traffic; traffic control

1. Introduction

Travel time is widely regarded as an important measure of the quality of mobility on a road network. The total travel time of vehicles can be used to reflect the performance of the road network and is of great interest for road authorities. The individual travel time is an important quality of a journey for travelers who need to make decisions on their travel choices, e.g., route choice, mode choice and departure time choice. Especially, for travelers the variation of travel times is also an important quality measure. Also for road managers travel time reliability is becoming an important criterion for evaluation of traffic situations and the choice of infrastructural and traffic management measures.

Over the past decades, a bunch of travel time estimation and prediction models focusing on mean travel times have been proposed, for instance, model-based approaches (Chen et al. 2001; Chien et al. 2002; Kwon et al. 2005) and data-driven approaches (Innamaa 2005; van Hinsbergen et al. 2009; van Lint et al. 2005). These models perform

quite well on freeways. The assumption behind both approaches is that travel times are determined by traffic states along the route. However, the mechanism on urban roads is very different from that on freeways. Vehicles traveling on urban roads are subjected to intersection delays due to queues and traffic control, and mid-link delay caused by turning vehicles from cross streets, bus maneuvers at bus stops, parking vehicles along the roadside, crossing pedestrians and cyclists, etc. Moreover, intersection delays vary with effects of stochastic properties of traffic flow, stochastic arrivals and departures at the signalized intersection, and variations in the traffic control as well. These partly stochastic factors are not independent but rather cooperate with each other. As a result, delays are uncertain given known traffic condition (traffic flow) and traffic control scheme.

Of course, such influences can be simulated with a microscopic simulation program. The limitations of such an approach is that there is no direct relation between the parameters that can be controlled, like signal settings, and the traffic performance measures like a travel time distribution. The influence of control measures can be analyzed by repeated simulation runs in a heuristic search procedure (e.g. Yun and Park 2006) or by the derivation of a meta model which describes the behavior of certain performance measures as function of control parameters. This was done, for example, for a single intersection by Webster (1958) a long time ago and recently for whole networks by Osario (2015). Such meta models can give the heuristic relation between control parameters and performance measures, like travel time, delay and reliability. A disadvantage of the meta model approach it is a ‘black box’ because the physical process that determines the traffic performance is not visible in the model.

As an example of the role of the physical process determining the traffic performance we can look at the free flow travel time. This is basically determined by the distance and the free flow speed. The free flow speed is again determined by the speed limit, vehicle composition, spacing between intersections, lane width, etc. (Yusuf 2010) and, of course by the preference of the drivers. Therefore, the free flow travel time given known travel distance is not a constant value but variable depending on external and internal factors,. The results of all these factors is that for a given link or route travel time within a certain time period, travel times are variable and a certain travel time distribution can be observed. The key question is how to model this traffic process in such a way that the influence of control and management measures can directly be seen in an analytical relation between internal and external parameters and the performance.

The complexity of urban traffic has been recognized by more and more researchers recently. Therefore, different advanced modeling techniques and approaches have been developed to estimate or predict urban travel times. First of all empirical techniques have been developed to monitor urban travel times. Bhaskar et al. (Bhaskar et al. 2009; 2011) proposed a model to estimate average travel time by integrating cumulative plots from loop detectors and probe vehicle data. Skabardonis et al. (Skabardonis et al. 2005; 2008) applied shockwave theory to estimate the mean travel time on signalized roads. It is widely accepted that shockwave theory is able to capture the dynamics of traffic queuing process more realistically. Nevertheless, it fails to model stochasticity of traffic, especially on urban roads with intersections. Similarly, the Cell Transmission Model (CTM), which has been extensively applied to estimate or predict traffic states on

freeways, has the ability to capture the macroscopic features of traffic in both congested and uncongested conditions. Lo (Lo 2001) extended the CTM model for urban road network scenarios with signalized intersections. However, in CTM, the queue forms in a deterministic way which is not realistic in the urban context. Boel and Mihaylova (2006) and (Sumalee et al., 2011). developed stochastic versions of the CTM.

The state-space neural network (SSNN) model was first proposed by van Lint et al. (van Lint et al. 2005) to predict travel times on freeways. The prediction results are quite promising. The application of SSNN model to the urban road network is less successful due to the difficulties in prediction turning fractions at intersections and highly complex traffic conditions along the road as discussed by Liu (Liu 2008). Furthermore, the SSNN model also ignores the stochasticty of the traffic process.

Compared with average travel time estimation models for urban roads, very few urban travel time distribution models were proposed up to now. Guo et al. (Guo et al. 2010) developed a multi-state travel time distribution model, which provides the connection between the travel time distributions and the underlining traffic states. Similar work can also be found in Loustau et al.(Loustau et al. 2010). Ramezani and Geroliminis (Ramezani and Geroliminis 2012) proposed a route travel time distribution model by applying a Markov chain procedure. They investigated how to deal with correlations in travel times of consecutive links when link travel time distributions are merged to route travel time distributions. The validity of their model is confirmed by both field and simulation tests. The above reviewed research on travel time distribution mainly focuses on applying certain statistical distributions to the observed travel times. The influence of

different traffic processes and traffic control schemes on travel time variability is not explicitly considered or modeled. Hofleitner et al. (2012) recently developed a method to estimate the dynamics of travel time distributions from scarce probe vehicle data. They find empirical travel time distributions that can be used for monitoring purpose. However, their method cannot help to choose and optimize traffic management measures, because the calculated travel time distribution has a descriptive character and does not contain the influence of control measures.

In order to investigate how traffic flows and different signal control schemes influence arterial travel times, Lu et al. (Lu and Chang 2012) proposed a travel time model to estimate the arterial travel time and its variability by tracking the evolution of a queue on each link in a probabilistic way. In (Cui et al. 2013) , the expected arterial travel time and its variance are estimated considering the probability of a certain traffic condition vehicles encounter within a signal cycle. However, the stochastic processes at intersections and stochastic properties of traffic flow are not explicitly modeled in their research.

As shown in (Zheng and van Zuylen 2010), the variability of travel time between vehicles is large and the statistical distributions of travel times in different traffic conditions are strongly overlapping: an observed travel time can be the same for over-saturated conditions and light traffic conditions. The consequence is that travel times alone are not sufficient indicators of the status of the traffic. This uncertainty of travel time is largely caused by the stochastic processes (i.e. stochastic arrivals and departures) at intersections. Besides, the signal control at intersections has significant influence on

the travel time, especially in the case that two intersections are shortly distanced. If two intersections are not well coordinated, the spillback phenomenon can occur, blocking the upstream intersection. In the literature ,e,g., in (Wu and Liu 2011; Geroliminis and Skabardonis 2011), the spillback phenomenon is usually modeled by applying shockwave theory in a deterministic way without considering stochastic properties of traffic flow. Van Zuylen and Hoogendoorn (van Zuylen and Hoogendoorn 2006) developed a probabilistic model for queue length based on a Markov queuing model combined with first order traffic flow model, but they did not apply this to the spill back process. The character of urban travel times is represented by a specific distribution which can be influenced by different traffic processes (e.g., traffic flow, traffic control). The understanding of fundamental mechanisms of urban travel times helps to better deal with travel time variability, predicting travel time variability and, furthermore, influence travel time variability.

Many factors can influence the urban travel time and its variability. For the optimization of travel time and the reduction of the variability, a model of the mechanisms that influence these characteristics is needed. A complete analysis of all these factors on resulting travel times seems unrealistic. On urban signalized arterial roads, delay at intersections constitutes a large part of the total delay vehicles experience and therefore has a significant impact on the travel time. The main contribution of this work is the development of a theoretical travel time distribution model for urban signalized arterial roads, which is composed of a delay distribution and a free flow travel time distribution. This proposed model, which takes stochastic properties of traffic flow, stochastic arrivals

and departures, traffic control scheme, and the variability of free flow travel time into account, is based on the underlining traffic mechanisms and can be generalized for different traffic conditions. The spillback phenomenon is explicitly modeled by applying the shockwave theory in a probabilistic way. (see section 2 and section 3). In section 4, the model estimated travel time distributions are compared with those generated from a VISSIM simulation model and field GPS data. Section 5 discussed the possible extension of the delay distribution model to a corridor with more than two intersections. Section 6 gives a concluding discussion on the main findings and provides some final remarks.

2. Link travel time distribution

2.1 Definition of the link travel time

The complete link travel time here is defined as the travel time when the vehicle passes the stop line of the upstream intersection until it crosses the stop line of the downstream intersection as illustrated in Figure 1. The link travel time is expressed as:

$$TT = t_{exit} - t_{entry} \tag{1}$$

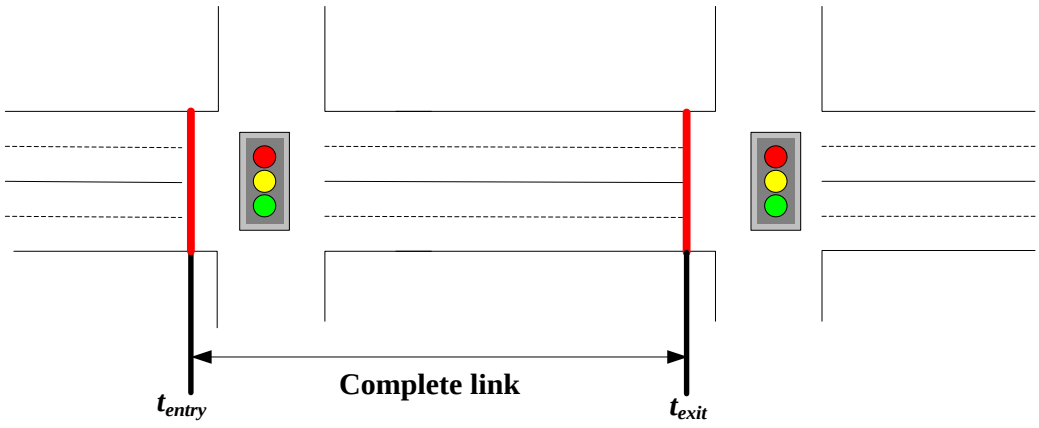

Figure 1 Schematic representation of an urban link

2.2 Components of urban link travel time

Basically, the travel time vehicles experience on a certain link i can be subdivided into two components:

$$TT_i(t) = TT_i^{\,f}(t) + W_i(t) \tag{2}$$

Where $TT_i^{\,f}(t)$ represents the free flow travel time at time instant t on link i, calculated from stop line to stop line. It is further calculated as the link length D_i divided by the free flow speed u_f:

$$TT_i^{\,f}(t) = \frac{D_i}{u_f} \tag{3}$$

The free flow speed varies with different driving behavior, speed limit, spacing between intersections, vehicle composition, weather conditions, etc. Therefore, the free flow travel time is not a constant value. $W_i(t)$ represents the delay vehicles experience when departing at time instant t. Delays vehicles encountered on an urban trip can be caused by different factors, e.g., bus maneuvers at bus stops, vehicles parking along the roadside, crossing pedestrians and cyclists, traffic control and queues at intersections. Among all these factors, the delay at intersections due to the queue and traffic control constitutes a large part of the total delay. In this paper, we mainly consider the delay at intersections. The time spent while driving in the queue towards the stop line is attributed to the delay as far as it is more than the time needed for driving with free speed. This is equivalent to the assumption that the queues are vertical at stop line.

2.3 Derivation of delay distribution for isolated intersections

The mathematical model for the delay distribution at an isolated intersection has been derived and published by the authors (Zheng and van Zuylen 2010), Viti and van Zuylen (Viti and van Zuylen 2010) and Olszewski (Olszewski, 1994). The model contains two mechanisms:

1. the (random) arrival process at the signal giving a block shaped delay function with a delta function at zero delay (figure 2a),
2. the overflow queue, the queue at the end of the green phase due to structural or accidental oversaturation of the green phase.

In the undersaturated condition, when vehicles arrive with a constant headway at the beginning of the red time, delay equals to the red time plus the time to release the initial overflow queue and decreases linearly until zero. While in the oversaturated condition, some or all arriving vehicles need to wait for another cycle or more cycles to depart due to the large overflow queue in front of it (figure 2b). As discussed in Zheng and van Zuylen (Zheng et al., 2010), the delay distribution in undersaturated conditions consists of a Dirac delta function and a box shaped function. The Dirac function in the distribution model describes the vehicles that pass the intersection without delay at the end of the green time. The box functions represent the vehicles that experience delay. For the oversaturated condition, the probability distribution consists of several box shaped functions that may overlap. The mathematical formulation of the model is as follows:

$$P_d(w|n_i) = \alpha(n_0)\delta(w) + \sum_N \beta B(w, w_{2N+1}(n_0), w_{2N+2}(n_0)) \quad (4)$$

Where $P_d\,(w|n_0)$ denotes the probability of a certain delay 'w' given a fixed overflow queue n_0; N is the number of extra red time that arriving vehicles need to wait for, which can be derived as:

$$N = \left\lfloor \frac{qt + n_0 + 1}{s\tau_g} \right\rfloor \tag{5}$$

t is the vehicle arrival moment at (the vertical queue before) the intersection. The floor $\lfloor\ \rfloor$ is used to indicate the integer value of the expression inside the brackets. The minimum and maximum number of extra red time can be derived from Eq. (5):

$$N_{\min} = \left\lfloor \frac{n_0 + 1}{s\tau_g} \right\rfloor \tag{6}$$

$$N_{\max} = \left\lfloor \frac{q\tau_C + n_0 + 1}{s\tau_g} \right\rfloor \tag{7}$$

$\delta(w)$ is the Dirac delta function with the following properties:

$$\begin{aligned} &\delta(w) = 0, \qquad if \quad w \neq 0 \\ &\int_{-\infty}^{+\infty} f(w)\delta(w)dw = f(0) \end{aligned} \tag{8}$$

$B(w, w_{2N+1}, w_{2N+2})$ is a box function with the property:

$$B(w, w_{2N+1}, w_{2N+2}) = \begin{cases} 1 & w_{2N+1} < w < w_{2N+2} \\ 0 & otherwise \end{cases} \tag{9}$$

w_{2N+1}, w_{2N+2} are delay boundaries determined by flow, overflow queue, signal timing (e.g., red phase, cycle time and coordination of intersections in case of an urban corridor):

$$W_{2N+1} = \begin{cases} (N+1)\tau_C + \dfrac{n_0 + 1 - (N+1)s\tau_g}{q} & N\min \le N < N\max \\ (N+1)\tau_r + \dfrac{n_0 + 1}{s} - \tau_C(1 - \dfrac{q}{s}) & N = N\max \end{cases} \tag{10}$$

$$W_{2N+2} = \begin{cases} (1+N)\tau_r + \dfrac{n_0+1}{s} & N = N\min \\ N\tau_C + \tau_r + \dfrac{n_0+1-Ns\tau_g}{q} & N\min < N \le N\max \end{cases} \tag{11}$$

α and β are model parameters following from the traffic state, e.g. the flow q, overflow queue n_0, the red phase τ_r and cycle time τ_C with:

$$\alpha = \max(1 - \frac{\tau_r + \frac{(n_0+1)}{s}}{\tau_C(1-\frac{q}{s})}, 0) \quad , \quad \beta = \frac{1}{\tau_C(1-\frac{q}{s})}$$

Where, s is the saturation flow rate.

In reality, the overflow queue is not deterministic but stochastic (Viti et al., 2010). For the given probability distribution of overflow queue $p(n_0)$, the expected delay probability distribution is calculated as a weighted sum of probability functions:

$$P_d(w) = \sum_{n_0=0}^{\infty} P_d(w|n_0)\, p(n_0) \tag{12}$$

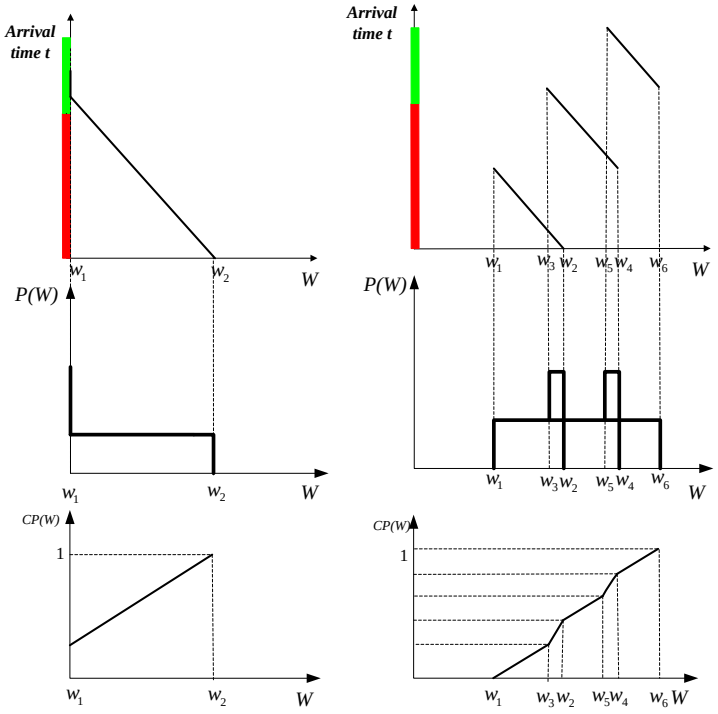

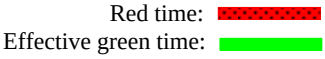

(a)Undersaturated condition (b) Oversaturated condition

Figure 2 Delay probability distribution and cumulative distribution for both undersaturated and oversaturated conditions at an isolated intersection.

2.4 Derivation of a single link travel time distribution

Case 1: constant free flow travel time

The free flow travel time can be estimated by simply assuming a constant free flow speed (e.g., the speed limit). In that case, the free flow travel time is a constant value. The delay vehicles experience at the signalized intersection is derived based on the vertical queue. This does not have a relevant influence on the final calculation of the total link travel time for the case of undersaturated conditions or slightly oversaturated conditions as long as no spill back is happening. The probability of a certain link/trip travel time τ, $P(\tau)$ can then be seen as the shifted probability of a certain delay w as:

$$P(\tau) = P_d(\tau - \tau_f) \tag{13}$$

where, τ_f is the free flow link travel time; $P(\tau)$ is the probability of a certain link travel time τ ($\tau = w + \tau_f$); $P_d(w)$ is the probability of a given delay w.

Case 2: stochastic free flow travel time

However, the free flow travel time in most cases is not a constant value. Instead, the free flow travel time has a certain probability distribution. As for an isolated intersection, the delay distribution shown above deals with a single intersection with uniform arrivals with stochastic arrival rates. The influence of the variable free flow travel times can be represented by combining the free flow travel time with the delay distribution as:

$$P(\tau) = \int_0^{\tau} P_d(\tau - \tau_f \mid \tau_f) P_f(\tau_f) d\tau_f \tag{14}$$

Where $P_f(\tau_f)$ denotes the free flow travel time distribution; $P_d(w|\tau_f)$ denotes the conditional probability of the delay w given a certain free flow travel time τ_f. For a given travel time τ ($\tau=w+\tau_f$), this conditional probability can also be formulated as:

$$P_d\left(w \middle| \tau_f\right) = P_d\left(\tau - \tau_f \middle| \tau_f\right) \tag{15}$$

Where $P_d(w)$ is given by Eq.(12).

For the case that both the delay probability distribution and free flow travel time distribution are represented as discrete, the link travel time distribution can be modified as:

$$P(\tau) = \sum_{\tau_f=0}^{\tau} P_d\left(\tau - \tau_f \middle| \tau_f\right) P_f\left(\tau_f\right) \tag{16}$$

3. Trip travel time distribution

3.1 Delay at adjacent intersections

In order to derive the delay distribution for an urban trip with a group of signals, we limit ourselves by the following conditions:

1) Fixed-time controlled intersections are considered in a single trip.

2) The acceleration and deceleration effects are not explicitly considered and assumed to be part of the delay. The concepts of effective green, effective red and saturation flows are used instead. E.g., the effective green and saturation flow determine the moment that a vehicle passes the stop line, which is the end of its delay.

3) The arrival times of vehicles are uniformly distributed within one cycle which can be considered as the average arrival rate of the cycle. Note that the arrival rates may vary from cycle to cycle under this assumption according to a certain statistical distribution, e.g. a Poisson distribution. Van Zuylen and Viti (van Zuylen and Viti 2006) showed that the assumption of uniform arrivals does not limit the validity of the calculation of delays.

4) Platoon dispersion is not considered within one cycle between two adjacent intersections.

5) The mid-link delay caused by bus maneuvers at bus stops and vehicles' parking etc. along the roadside is not considered.

As for fixed-time control, the coordination scheme among intersections has a big influence on the delay. Figure 3 (a) and (b) illustrates different offset settings for two fixed-time controlled intersections. For the convenience of modeling, we assume that both intersections have the same cycle time τ_C, effective green time τ_g and red time τ_r. These assumptions can be relaxed to different effective green times between consecutive intersections. The derivations in the following sections are all based on the assumption of the same cycle time and effective green time between two consecutive intersections. The offset τ_{off} between two intersections is defined as:

$$\tau_{off} = t_2 - t_1 \tag{17}$$

where t_1 is the beginning of effective green time at the upstream intersection and t_2 is the beginning of effective green time at the downstream intersection. The link length

between the two intersections is D; the free flow speed is u_f. Then the free flow link travel time is:

$$\tau_f = \frac{D}{u_f} \tag{18}$$

If two intersections are well coordinated, there is no mismatch between these two intersections. In the case that two intersections are not well coordinated, the mismatch of green time τ_m as illustrated in Figure 3 (a) (b) between the upstream intersection and the downstream intersection can be derived as:

$$\tau_m = \tau_f - \tau_{off} \tag{19}$$

Two types of mismatch can be found in reality as shown in Figure 3.

1) **Mismatch 1, early green:** As illustrated in Figure 3 (a), the start of the green phase at the downstream intersection is too early such that part of the green time is not utilized by the platoon. Hence, the mismatch between the two intersections is positive :

$$\tau_m = \tau_f - \tau_{off} > 0$$

Since the mismatch time is only utilized by the remaining queue from the previous cycle not by the vehicles departing from the upstream intersection right after the traffic light turns to green. The effective green time of the downstream intersection when vehicles can pass without delay is given by:

$$\tau_g' = \tau_g - \tau_m \tag{20}$$

2) **Mismatch 2, late green:** As illustrated in Figure 3 (b), the start of the green phase at the downstream intersection is too late so that vehicles departing directly after the start of the green time from the upstream intersection need to wait for the red time at the downstream intersection. Hence, the mismatch between the two intersections is negative:

$$\tau_m = \tau_f - \tau_{off} < 0$$

In this subsection, the delay vehicles experience when traversing the two consecutive intersections is analyzed and discussed according these two types of mismatch.

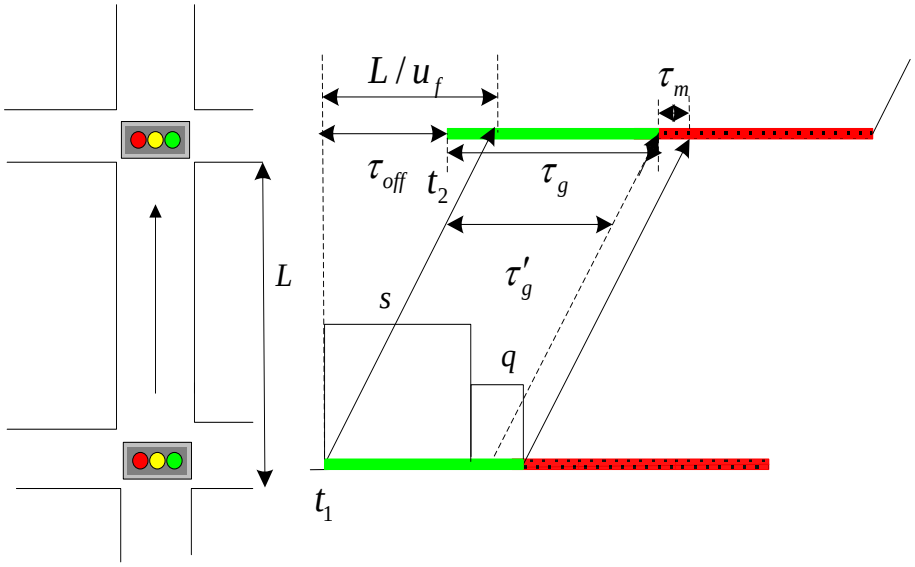

(a, early green)

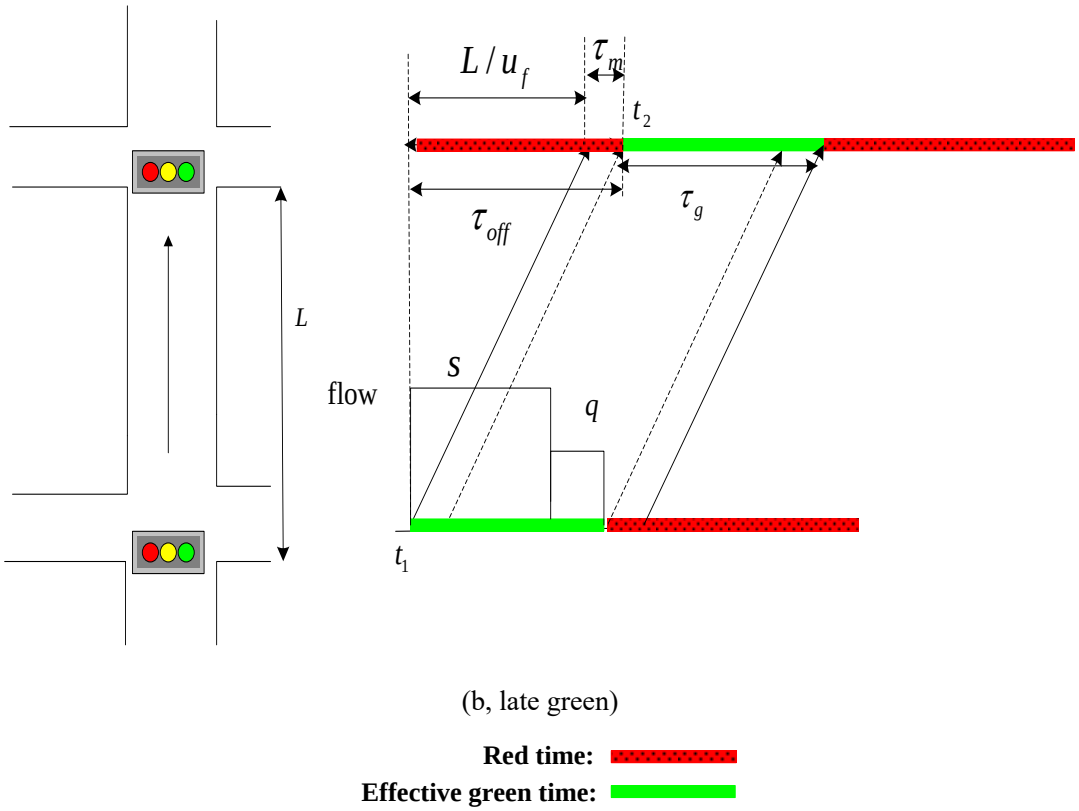

Figure 3 Offsets at adjacent intersections

3.1.1 Mismatch 1, early green

(1) When the upstream intersection is undersaturated

Figure 4 illustrates the delay that vehicles experience passing two signalized intersections. We assume that there is no oversaturation (filtered by the upstream intersection) at the downstream intersection. Depending on the arrival moment at both intersections, the initial overflow queue at the upstream intersection and offsets between two intersections, delay vehicles experience can be categorized into three cases:

Case 1: Figure 4 (a)

As shown in Figure 4 (a), vehicles leaving from the upstream intersection at time t_1

can pass the downstream intersection without delay. Vehicles departing from the first intersection after $t_1 + \tau_g'$ have to wait at the second intersection. The arrivals are first in a dense platoon determined by the saturation flow and after the saturated green time, the flow is determined by the arrival rate. When the vehicle arrives at the beginning of the red time t_0 at the upstream intersection, delay equals to the red time plus the time to release the initial overflow queue at the upstream intersection plus the arriving vehicle itself and decreases linearly until zero at the saturated green time instant which is given by:

$$t_{sat} = t_0 + \tau_r + \tau_{sat} \tag{21}$$

Where τ_r is the red time; τ_{sat} is the saturated green time period at the upstream intersection which is calculated as:

$$\tau_{sat} = \frac{\frac{q}{s}\tau_r + \frac{n_0 + 1}{s}}{1 - \frac{q}{s}} \tag{22}$$

Where n_0 is the overflow queue at the first intersection; s is the saturation flow rate and q is the arriving flow rate.

Vehicles arriving at the upstream intersection experience zero delay after t_{sat} up till $t_f = t_0 + \tau_r + \tau_g'$ as shown in Figure 4 (a) and after t_f, vehicles have to wait for the red time at the downstream intersection. The delay as a function of arrival time at the stop line of the upstream intersection can be determined as:

$$W(t|n_0)=\begin{cases}\tau_r+\dfrac{n_0+1}{s}-(1-\dfrac{q}{s})(t-t_0) & t_0\le t\le t_{sat}\\ 0 & t_{sat}<t\le t_f\\ \tau_r-(1-\dfrac{q}{s})(t-t_f) & t>t_f\end{cases} \tag{23}$$

Case 2: Figure 4 (b)

As shown in Figure 4 (b), when the initial overflow queue becomes larger such that vehicles arriving the upstream intersection at time t_h before the end of the saturated green time t_{sat} have to wait for the red time at the downstream intersection. The moment t_h is given by:

$$n_0+q(t_h-t_0)+1=s\tau_g'$$

$$\text{i.e.}\quad t_h=t_0+\frac{s\tau_g'-n_0-1}{q} \tag{24}$$

Vehicles arriving before t_h only have delay at the upstream intersection and after t_h, vehicles need to wait at the downstream intersection. For this case, delay as a function of arrival time at the stop line of the upstream intersection can be calculated as:

$$W(t|n_0)=\begin{cases}\tau_r+\dfrac{n_0+1}{s}-(1-\dfrac{q}{s})(t-t_0), & t\le t_h\\ 2\tau_r+\dfrac{n_0+1}{s}-(1-\dfrac{q}{s})(t-t_0), & t>t_h\end{cases} \tag{25}$$

Case 3: Figure 4 **(c)**

As shown in Figure 4 (c), if the initial overflow queue departing from the upstream intersection can be so large that it can't leave the downstream intersection completely within the green time τ_g'. For this case, the vehicle arriving right after the start of the red

time at the upstream intersection needs to wait for the red time at the downstream intersection because of the long overflow queue which is given by:

$$n_0 + 1 \geq s\tau_g'$$
$$n_0 \geq s\tau_g' - 1$$

The delay vehicles experience can be calculated as:

$$W\left(t \middle| n_0\right) = 2\tau_r + \frac{n_0 + 1}{s} - (1 - \frac{q}{s})(t - t_0) \tag{26}$$

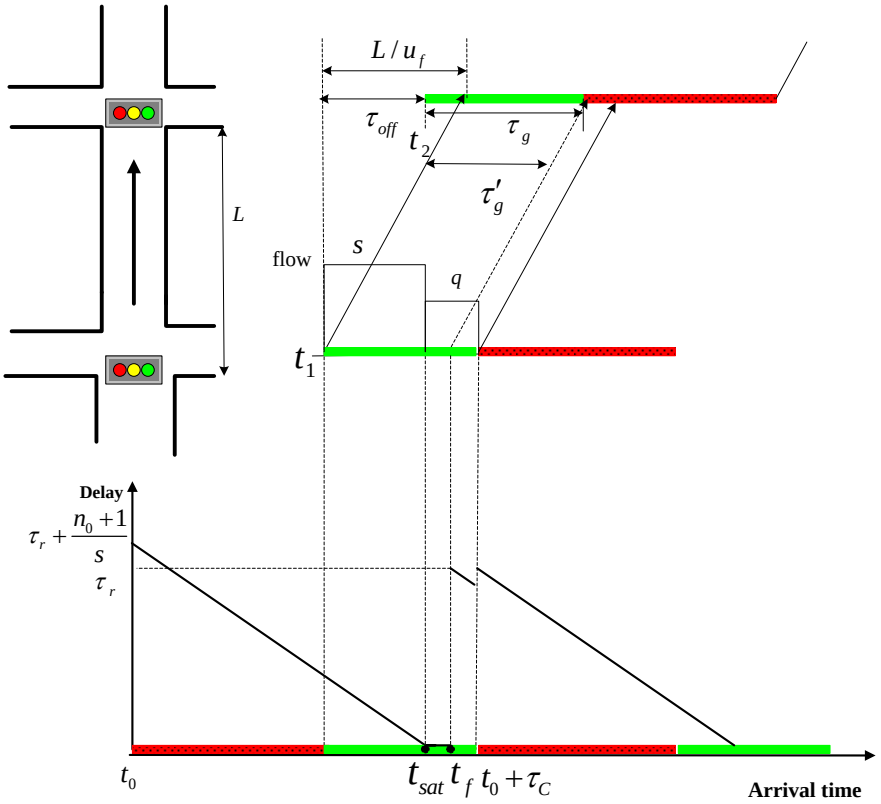

(a)

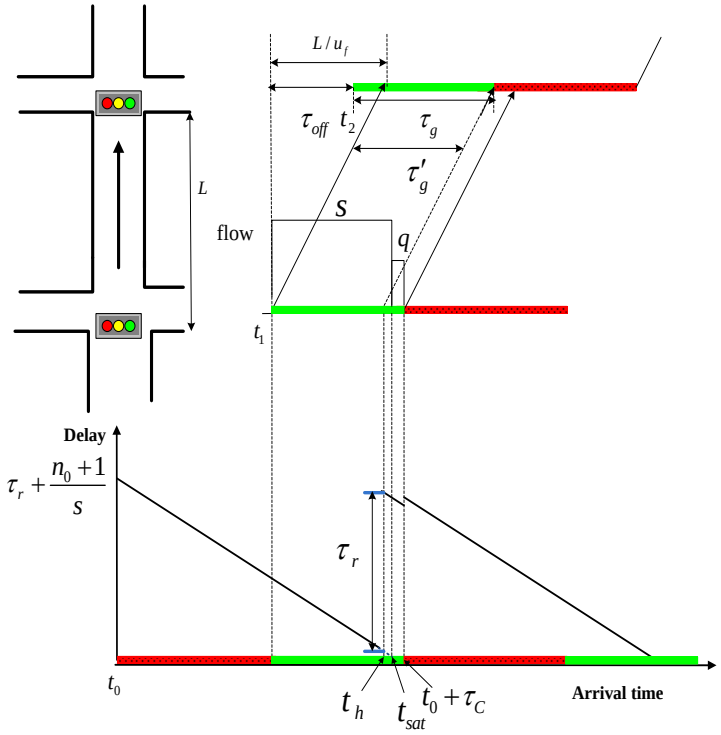

(b)

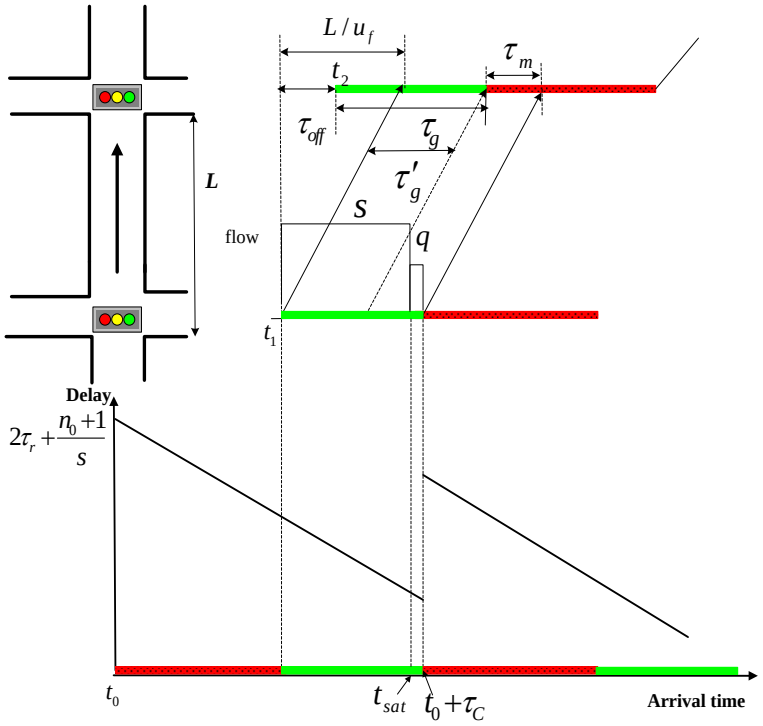

(c)

Figure 4 Delay as a function of arrival time for two adjacent intersections in the undersaturated condition (Mismatch 1, early green)

(2) When the upstream intersection is oversaturated

When the initial overflow queue at the upstream intersection is larger than a certain threshold, the green phase becomes oversaturated. The question whether an arriving vehicle has to wait for a next cycle to depart, depends on the number of vehicles that arrived before this one in the cycle plus the initial overflow queue. As soon as this quantity exceeds the number of vehicles that can depart in the (remaining) green time, the vehicle has to wait for a following cycle or even more cycles at the upstream intersection. On the other hand, whether the vehicle departing from the upstream intersection needs to wait for the red time at the downstream intersection depends on the number of vehicles in front of this vehicle departing from the upstream intersection in the same cycle. If this quantity exceeds the number of vehicles that can depart from the downstream intersection in the effective green time, the vehicle needs to wait for the red time again at the downstream intersection. The general expressions can be derived as:

$$W\left(t\middle|n_0\right)=\begin{cases}\{\tau_r+\dfrac{n_0+1}{s}+\left\lfloor\dfrac{n_0+q(t-t_0)+1}{st_g}\right\rfloor\tau_r\}-(1-\dfrac{q}{s})(t-t_0), & if\ n_0+q(t-t_0)+1-\left\lfloor\dfrac{n_0+q(t-t_0)+1}{s\tau_g}\right\rfloor s\tau_g<s\tau_g' \\ \{2\tau_r+\dfrac{n_0+1}{s}+\left\lfloor\dfrac{n_0+q(t-t_0)+1}{st_g}\right\rfloor\tau_r\}-(1-\dfrac{q}{s})(t-t_0), & else\end{cases} \tag{27}$$

3.1.2 Mismatch 2, late green

For the case of late green, a vehicle leaving from the upstream intersection has to wait for the red light at the downstream intersection. Spillback could occur especially when two intersections are shortly distanced. In the following, four cases are discussed.

(1) When the upstream intersection is undersaturated

Case 1: The queue spills back from the downstream intersection

When the effective green period starts, vehicles leave at a saturation flow rate s until the saturated green time τ_{sat} which is given by Eq. (22). Afterwards, vehicles depart at the arrival flow rate q during the remaining green time. If the front of the queue does not meet the back of the queue, while the back of the queue exceeds the downstream link, a spillback queue can be observed (see Figure 5 (a)). The moment when spillback happens, i.e. the moment that the back of the queue reaches the upstream intersection, can be derived as:

$$t_{spillback} = t_0 + \tau_r + \tau_{sat} + \left(\frac{D}{l} - s\tau_{sat} \right) / q \tag{28}$$

Where t_0 is the start of the red time at the upstream intersection; D is the link length between the upstream intersection and the downstream intersection; l is the average effective length of a vehicle in a queue, which can be estimated as the length of a queue divided by the number of vehicles in the queue.

As shown in Figure 5 (a) and Figure 6 (a), when vehicles arrive at moment t before $t_{spillback}$, the delay at the upstream and the downstream intersections can be determined as:

$$W(t \left| n_0 \right.) = \tau_r + \tau_m + \frac{n_0 + 1}{s} - (1 - \frac{q}{s})(t - t_o), \qquad t < t_{spillback} \tag{29}$$

After $t_{spillback}$, the delay can be calculated as:

$$W(t \left| n_0 \right.) = \tau_C + \tau_r + \tau_m - \frac{D}{ls} + \frac{n_0 + 1}{s} - (1 - \frac{q}{s})(t - t_0), \qquad t \geq t_{spillback} \tag{30}$$

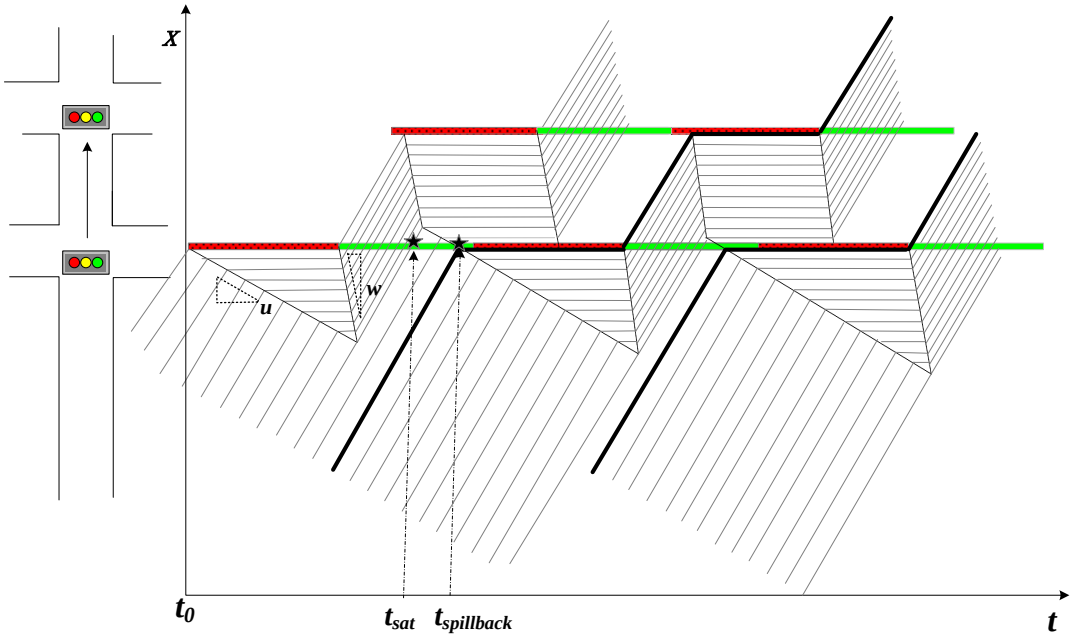

Figure 5 Trajectories of vehicles passing two intersections with spillback (The upstream intersection is under-saturated)

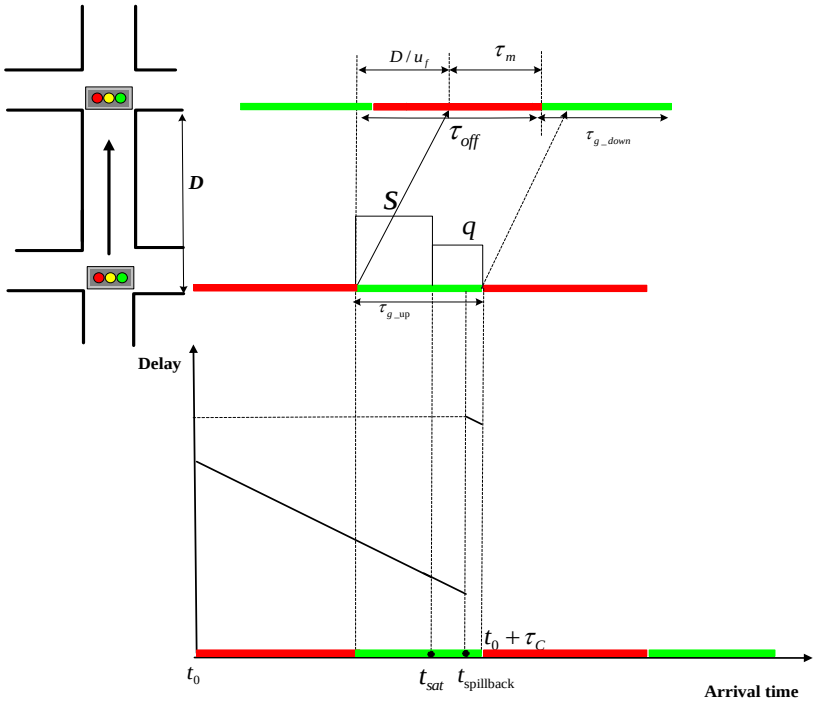

Figure 6 Delay as a function of arrival time for two adjacent intersections in the under-saturated condition with spillback

Case 2: No spillback happens from the downstream intersection (see Figure 7)

In this case, if the number of vehicles leaving from the upstream intersection during the effective green time of the upstream intersection can depart from the downstream

intersection during the effective green time of the downstream intersection as shown in figure 7 (a), delay as a function of arrival time at the stop line of the upstream intersection can be derived as:

$$W(t\left|n_0\right.) = \tau_r + \tau_m + \frac{n_0+1}{s} - (1-\frac{q}{s})(t-t_0) \tag{31}$$

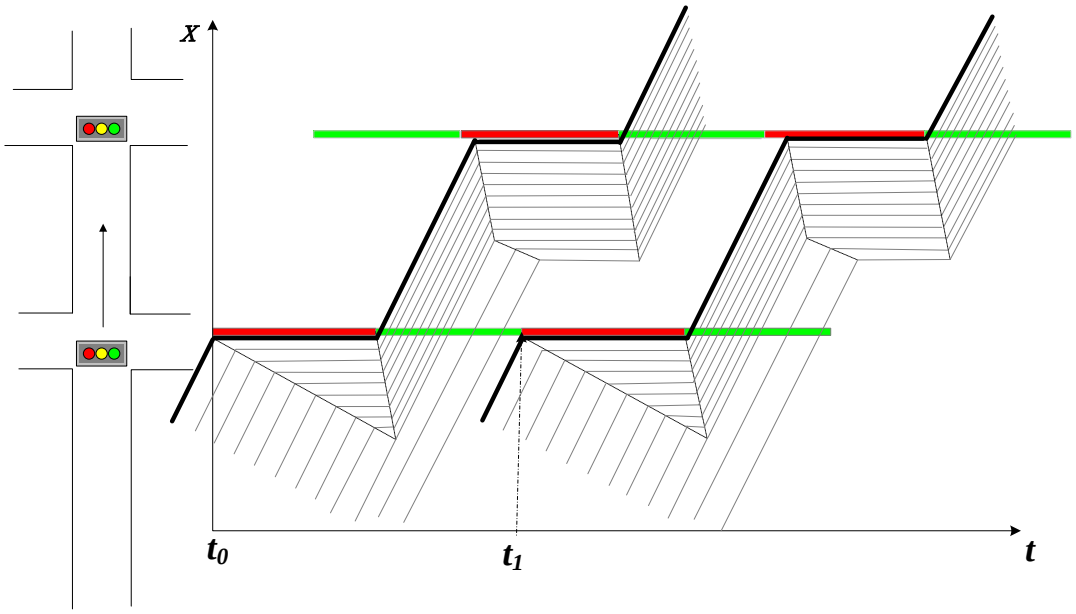

Figure 7 Trajectories of vehicles passing two intersections without spillback (The upstream intersection is under-saturated)

(2) When the upstream intersection is over-saturated

The initial overflow queue at the upstream intersection is large and the traffic demand is high such that the green phase becomes over-saturated. Similarly, two cases can be identified:

Case 3: Queue spills back from the downstream intersection

As illustrated in Figure 8, vehicles arriving at the upstream intersection have to wait for extra red times plus the green times blocked by the spillback queue. Delay as a

function of arrival time can be determined as:

$$W\left(t\middle|n_0\right)=\tau_r+\tau_m+\frac{n_0+1}{s}+\left\lfloor\frac{n_0+q(t-t_0)+1}{\frac{D}{l}}\right\rfloor\left(\tau_C-\frac{D}{ls}\right)-(1-\frac{q}{s})(t-t_o) \tag{32}$$

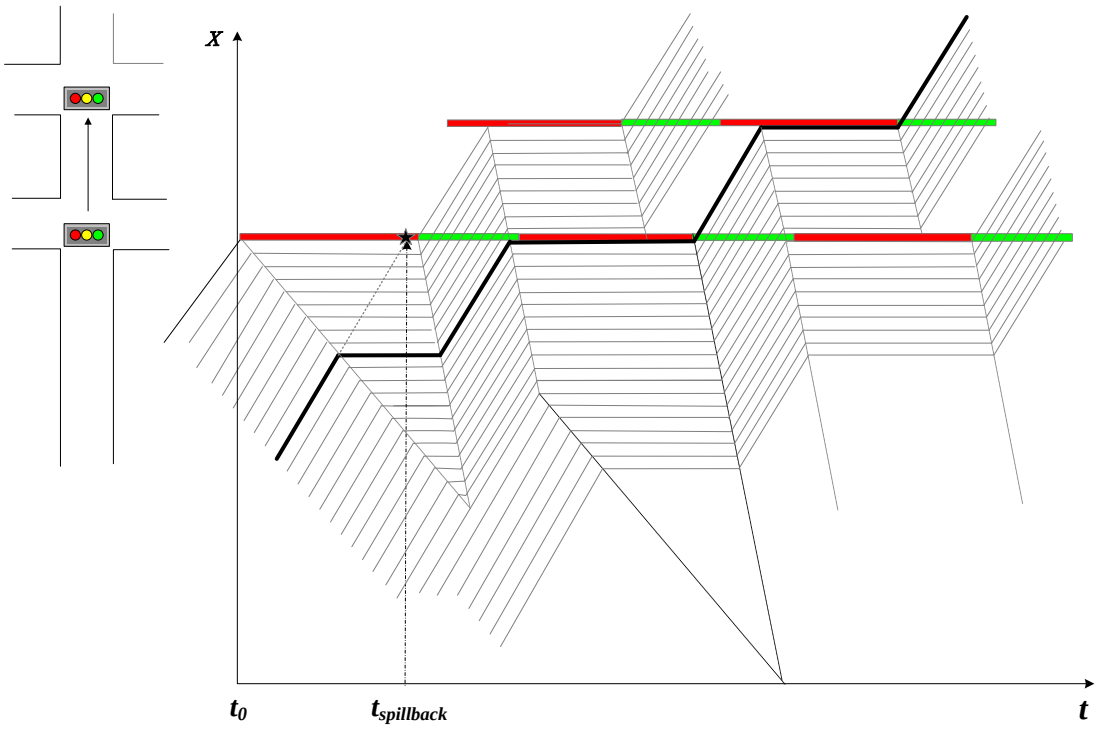

Figure 8 Trajectories of vehicles passing two intersections with spillback (The upstream intersection is over-saturated)

Case 4: No spillback from the downstream intersection

As shown in Figure 9, the arriving vehicle has to wait for extra red times at the upstream intersection due to the large initial overflow queue and the high traffic demand. On the other hand, vehicles departing from the upstream intersection during the green time period need to wait for the mismatch time period 'τ_m' at the downstream intersection. Delay as a function of arrival time can be deduced as:

$$W(t|n_0) = \tau_r + \tau_m + \frac{n_0 + 1}{s} + \left\lfloor \frac{n_0 + q(t - t_0)}{s\tau_g} \right\rfloor \tau_r - (1 - \frac{q}{s})(t - t_o) \quad (33)$$

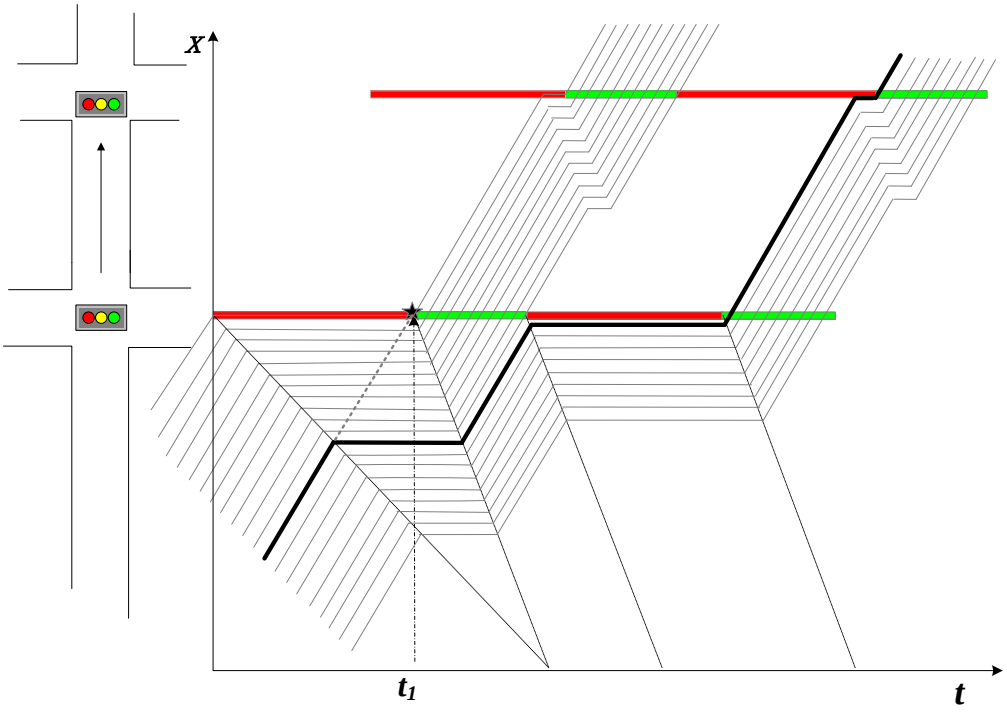

Figure 9 Trajectories of vehicles passing two intersections without spillback (The upstream intersection is over-saturated)

3.2 Delay distribution for adjacent intersections

The delay as function of the arrival time at the upstream intersection for two types of mismatch both in the undersaturated condition and oversaturated condition has been discussed in the previous subsection. In this subsection, the travel time distribution model for two consecutive fixed-time controlled intersections, taking the stochastic overflow queue in the first intersection and different mismatches between these two intersections into account, is developed.

3.2.1 Delay distribution with an initial deterministic queue

(1) Mismatch 1: early green

The delay as a function of arrival time at the upstream intersection both for the undersaturated condition and oversaturated condition can be derived according to Equations (23), (25), (26) and (27). As for the oversaturated condition, the number of extra red times that a vehicle arriving at time t needs to wait at the upstream intersection can be directly derived from Eq. (27). The more generic expression is:

$$N = \left\lfloor \frac{q(t - t_0) + n_0 + 1}{s\tau_g} \right\rfloor \tag{34}$$

From Equation (34), we can see that when a vehicle arrives within the time interval of one cycle time, the minimum number of extra red times this vehicle needs to wait at the upstream intersection can be derived as:

$$N_{\min} = \left\lfloor \frac{n_0 + 1}{s\tau_g} \right\rfloor \tag{35}$$

And the maximum number of extra red times is given by:

$$N_{\max} = \left\lfloor \frac{q\tau_C + n_0 + 1}{s\tau_g} \right\rfloor \tag{36}$$

If the value within $\lfloor \ \rfloor$ is an integer, the maximum delay will be experienced by the vehicle arriving at the end of the cycle. Otherwise, the maximum delay will appear before the end of the cycle ($t < t_0 + \tau_C$) in oversaturated conditions.

Whether vehicles need to wait for the red time at the downstream intersection depends on whether the number of vehicles in front of this vehicle plus the vehicle itself can be released within the green time τ_g' at the downstream intersection.

1) If $0 \le n_0 + q(t-t_0) + 1 - \left\lfloor \frac{n_0 + q(t-t_0)+1}{s\tau_g} \right\rfloor s\tau_g < s\tau'_g$, vehicles experience no delay at the downstream intersection. Vehicles just experience delays at the upstream intersection. Given the initial moment of the calculation t_0, in our approach, it is the beginning of the red time. For this case, the transition moments (discontinuity of the delay as function of t_n) appear when:

$$n_0 + q(t_N - t_0) + 1 - Ns\tau_g = 0$$

Each transition moment can be derived as:

$$t_N = \begin{cases} t_0 & N = N_{\min} \\ t_0 + \dfrac{Ns\tau_g - n_0 - 1}{q} & N_{\min} < N \le N_{\max} \end{cases} \tag{37}$$

2) If $n_0 + q(t-t_0) + 1 - \left\lfloor \frac{n_0 + q(t-t_0)+1}{s\tau_{g\_up}} \right\rfloor s\tau_{g\_up} \ge s\tau'_{g\_down}$ vehicles experience delays at both the upstream and downstream intersections, the transition moments appear when:

$$n_0 + q(t'_N - t_0) + 1 - Ns\tau_{g\_up} = s\tau'_{g\_down}$$

Each transition moment can be expressed as:

$$t'_N = t_0 + \frac{Ns\tau_g + s\tau'_g - n_0 - 1}{q} \tag{38}$$

An example is shown in Figure10. The ‘star’ points are the transition moments when vehicles arriving at the stop line of the upstream intersection need to wait for another red phase at the upstream intersection. The dots are transition moments when vehicles arrive at the stop line of the upstream intersection will experience an extra delay of ‘red phase’ at the downstream intersection. The star transition moments lie on the decreasing trend

line starting from the dot transition moments in case two intersections have the same red time. However, if the upstream intersection and the downstream intersection have different red times, the star transition moments can be above or below the trend line. Figure 11 illustrates trajectories of vehicles passing two intersections. The bold solid lines indicate trajectories of vehicles arriving at the 'transition moments' which are 'dots' and 'stars' as shown in Figure 10. In the case of a vertical queue, the 'transition arrival moments't'_1, t_1 are extrapolated and the dotted lines are virtual trajectories of vehicles arriving at the stop line of the upstream intersection.

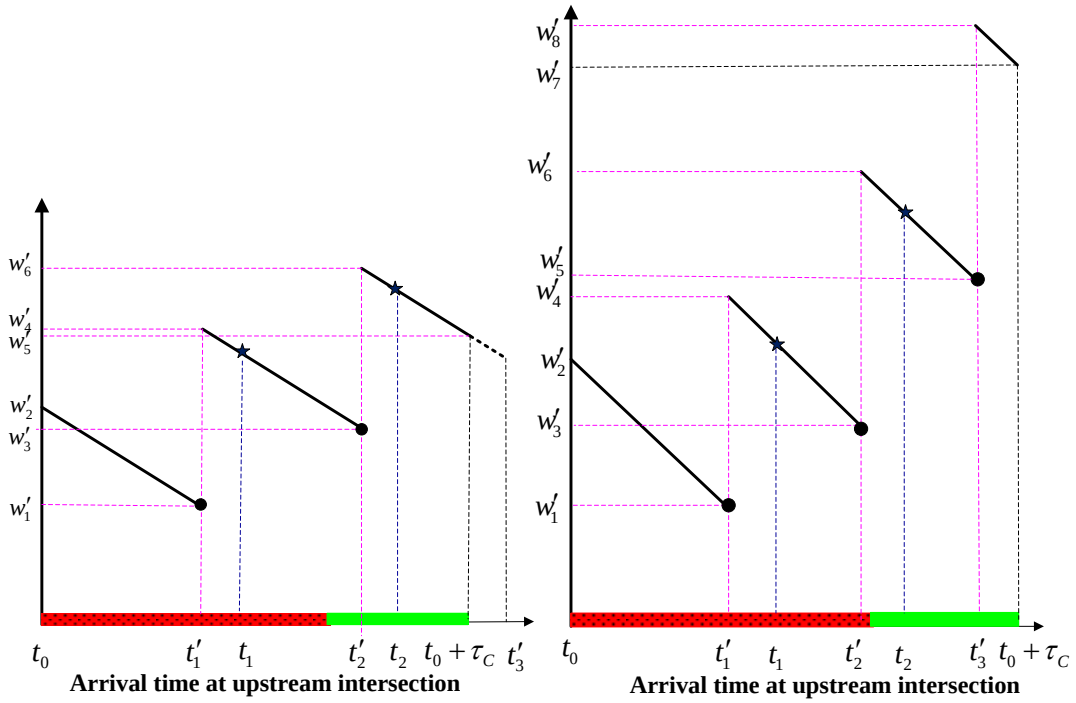

（a） $\dfrac{2s\tau_g + s\tau'_g - n_0 - 1}{q} > \tau_C$ （b） $\dfrac{2s\tau_g + s\tau'_g - n_0 - 1}{q} \le \tau_C$

Figure 10 Delay as a function of arrival time (at the stop line of the upstream intersection in the case of a vertical queue) in the oversaturated condition with the same red time for both intersections (Mismatch 1, early green)

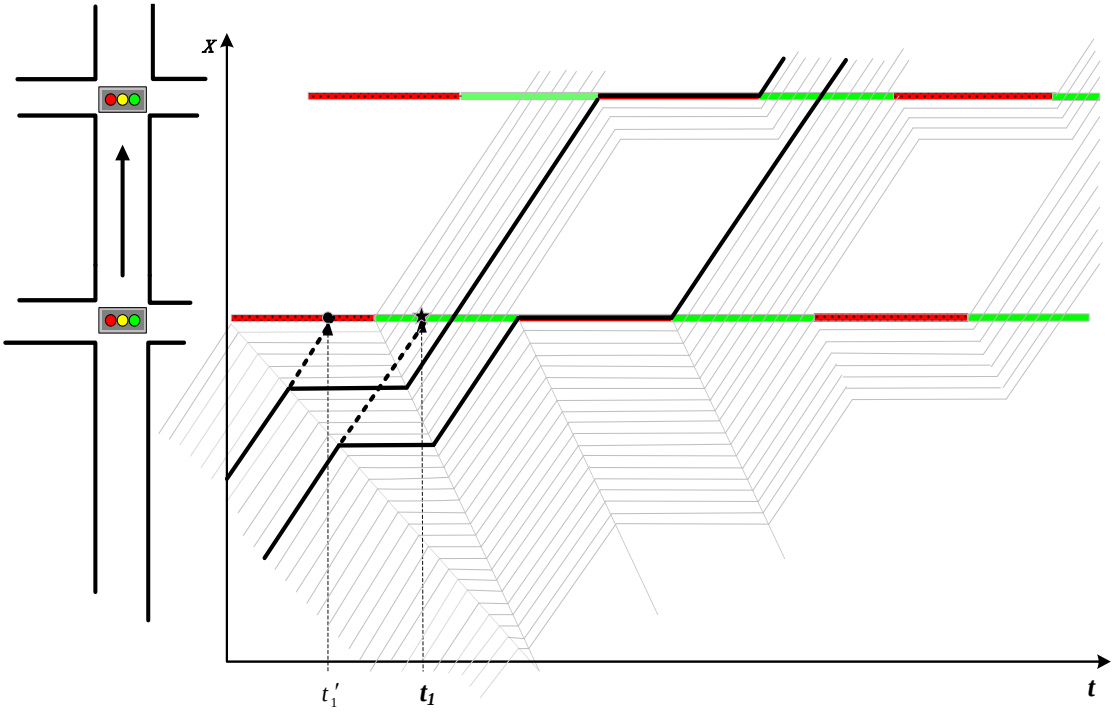

Figure 11 Trajectories of vehicles passing two intersections (Mismatch 1, early green)

According to Equation (27), delay at these transition moments can be calculated. Due to the complexity, the detailed deduction process of delays for different transition moments is not discussed in this paper. The general expressions of delay for these transition moments and the initial moment are given as follows:

(1) If $n_0+1-\left\lfloor \frac{n_0+1}{s\tau_g} \right\rfloor s\tau_g < s\tau_g'$ & $\frac{N_{\max}s\tau_g + s\tau_g' - n_0 - 1}{q} > \tau_C$:The first vehicle arriving right after the beginning of the red time can leave the downstream without delay and the last transition moment according to Equation (37) is larger than the cycle time (shown in Figure 10a), then delays at the transition moments are given by:

$$W_{2N+1} = \begin{cases} N\tau_C + \tau_r + \tau_g' - \frac{Ns\tau_g + s\tau_g' - n_0 - 1}{q} & N_{\min} \le N < N_{\max} \\ (N+1)\tau_r + \frac{n_0+1}{s} - \tau_C(1-\frac{q}{s}) & N = N_{\max} \end{cases} \tag{39a}$$

$$W_{2N+2}=\begin{cases}(N+1)\tau_r+\dfrac{n_0+1}{s} & N=N_{\min}\\ (N-1)\tau_C+2\tau_r+\tau_g'-\dfrac{(N-1)s\tau_g+s\tau_g'-n_0-1}{q} & N_{\min}<N\le N_{\max}\end{cases} \tag{39b}$$

(2) If $n_0+1-\left\lfloor\dfrac{n_0+1}{s\tau_g}\right\rfloor s\tau_g<s\tau_g'$ & $\dfrac{N_{\max}s\tau_g+s\tau_g'-n_0-1}{q}\le\tau_C$: The first vehicle arriving right after the beginning of the red time can leave the downstream without delay and the last transition moment according to Equation (37) is within the cycle time (shown in Figure 10 b), then delays at the transition moments are given by:

$$W_{2N+1}=\begin{cases}N\tau_C+\tau_r+\tau_g'-\dfrac{Ns\tau_g+s\tau_g'-n_0-1}{q}, & N_{\min}\le N\le N_{\max}\\ (N+1)\tau_r+\dfrac{n_0+1}{s}-\tau_C(1-\dfrac{q}{s}) & N=N_{\max}+1\end{cases} \tag{40a}$$

$$W_{2n+2}=\begin{cases}(N+1)\tau_r+\dfrac{n_0+1}{s} & N=N_{\min}\\ (N-1)\tau_C+2\tau_r+\tau_g'-\dfrac{(N-1)s\tau_g+s\tau_g'-n_0-1}{q} & N_{\min}<N\le N_{\max}+1\end{cases} \tag{40b}$$

(3) If $n_0+1-\left\lfloor\dfrac{n_0+1}{s\tau_g}\right\rfloor s\tau_g\ge s\tau_g'$ & $\dfrac{N_{\max}s\tau_g+s\tau_g'-n_0-1}{q}>\tau_C$: The initial overflow queue is so large that the first vehicle arriving right after the start of the red time at the upstream intersection has to wait for the red time at the downstream intersection plus the condition that the last transition moment according to Equation (38) is larger than the cycle time (shown in Figure 10 a). For this case, then delays at the transition moments are calculated as:

$$W_{2N+1}=\begin{cases} N\tau_C+\tau_r+\tau_g'-\dfrac{Ns\tau_g+s\tau_g'-n_0-1}{q} & N_{\min}+1\le N<N_{\max} \\ (N+1)\tau_r+\dfrac{n_0+1}{s}-\tau_C(1-\dfrac{q}{s}) & N=N_{\max} \end{cases} \tag{41a}$$

$$W_{2N+2}=\begin{cases} (N+1)\tau_r+\dfrac{n_0+1}{s} & N=N_{\min}+1 \\ (N-1)\tau_C+2\tau_r+\tau_g'-\dfrac{(N-1)s\tau_g+s\tau_g'-n_0-1}{q} & N_{\min}+1<N\le N_{\max} \end{cases} \tag{41b}$$

(4) If $n_0+1-\left\lfloor\dfrac{n_0+1}{s\tau_g}\right\rfloor s\tau_g\ge s\tau_g'$ & $\dfrac{N_{\max}s\tau_g+s\tau_g'-n_0-1}{q}\le\tau_C$: The initial overflow queue is so large that the first vehicle arriving right after the start of the red time at the upstream intersection has to wait for the red time at the downstream intersection plus the condition that the last transition moment according to Equation (38) is within the cycle time (shown in Figure 10 b). The delays at the transition moments for this case are given by:

$$W_{2N+1}=\begin{cases} N\tau_C+\tau_r+\tau_g'-\dfrac{Ns\tau_g+s\tau_g'-n_0-1}{q} & N_{\min}+1\le N\le N_{\max} \\ (N+1)\tau_r+\dfrac{n_0+1}{s}-\tau_C(1-\dfrac{q}{s}) & N=N_{\max}+1 \end{cases} \tag{42a}$$

$$W_{2N+2}=\begin{cases} (N+1)\tau_r+\dfrac{n_0+1}{s} & N=N_{\min}+1 \\ (N-1)\tau_C+2\tau_r+\tau_g'-\dfrac{(N-1)s\tau_g+s\tau_g'-n_0-1}{q} & N_{\min}+1<N\le N_{\max}+1 \end{cases} \tag{42b}$$

(2) Mismatch 2: late green

In case of mismatch 2, the delay as a function of arrival time at the upstream intersection with or without spillback both for the under-saturated condition and the over-

saturated condition can be derived according to Equations (29),(30), (31)-(33). In the over-saturated condition at the upstream intersection, the number of extra (red) times N that a vehicle arriving at time t has to wait at the upstream intersection can be derived from Equations (32) and (33). Depending whether there is spillback or not, the generic expressions can be derived as:

$$N = \left\lfloor \frac{q(t-t_0)+n_0+1}{s\tau_g} \right\rfloor, \quad no\ spillback \tag{43}$$

$$N_{spillback} = \left\lfloor \frac{n_0+q(t-t_0)+1}{\frac{D}{l}} \right\rfloor, \quad spillback \tag{44}$$

From the above equations, we can calculate the minimum number of extra (red) times this vehicle needs to wait at the upstream intersection as:

$$N_{\min} = \left\lfloor \frac{n_0+1}{s\tau_g} \right\rfloor, \quad no\ spillback \tag{45}$$

$$N_{\min\_spillback} = \left\lfloor \frac{n_0+1}{\frac{D}{l}} \right\rfloor, \quad spillback \tag{46}$$

Similarly, the maximum number of extra (red) times can be deduced as:

$$N_{\max} = \left\lfloor \frac{q\tau_C+n_0+1}{s\tau_g} \right\rfloor, \quad no\ spillback \tag{47}$$

$$N_{\max\_spillback} = \left\lfloor \frac{q\tau_C+n_0+1}{\frac{D}{l}} \right\rfloor, \quad spillback \tag{48}$$

Depending on the arrival moment at the upstream intersection, there is discontinuity of delay (transition moments) which can be observed as shown in Figure 12, where t_0, t_1, t_2, … are transition moments. These transition moments can be determined from Equations (32) and (33) as:

$$t_n = \begin{cases} t_0 & n = N_{\min} \\ t_0 + \dfrac{ns\tau_g - n_0 - 1}{q} & N_{\min} < n \le N_{\max} \end{cases}, \quad no\ spillback \tag{49}$$

$$t_{n\_spillback} = \begin{cases} t_0 & n = N_{\min\_spillback} \\ t_0 + \dfrac{\dfrac{nD}{l} - n_0 - 1}{q} & N_{\min\_spillback} < n \le N_{\max\_spillback} \end{cases}, \quad spillback \tag{50}$$

The mathematical expressions of delays at the transition moments, w_{2n+1} and w_{2n+2}, are given by Equations (51) - (54).

(1) If $\dfrac{s\tau_m}{k_j - k_s} > D$, spillback happens from the downstream intersection

$$w_{2n+1} = \begin{cases} n\tau_C + \tau_m + \tau_r + \dfrac{D}{ls} - \left[(n+1)\dfrac{D}{l} - n_0 - 1\right]/q & N_{\min\_spillback} \le n < N_{\max\_spillback} \\ n\left(\tau_C - \dfrac{D}{ls}\right) + \tau_m + \tau_r + \dfrac{n_0+1}{s} - \left(1 - \dfrac{q}{s}\right)\tau_C & n = N_{\max\_spillback} \end{cases} \tag{51}$$

$$w_{2n+2} = \begin{cases} \tau_r + \tau_m + n\left(\tau_C - \dfrac{D}{ls}\right) + \dfrac{n_0+1}{s} & n = N_{\min\_spillback} \\ n\tau_C + \tau_r + \tau_m - \left(\dfrac{nD}{l} - n_0 - 1\right)/q & N_{\min\_spillback} < n \le N_{\max\_spillback} \end{cases} \tag{52}$$

(2) If $\dfrac{s\tau_m}{k_j - k_s} \le D$, no spillback happens from the downstream intersection

$$w_{2n+1} = \begin{cases} (n+1)\tau_C + \tau_m - \dfrac{(n+1)s\tau_g - n_0 - 1}{q} & N_{\min} \le n < N_{\max} \\ (n+1)\tau_r + \tau_m + \dfrac{n_0+1}{s} - \left(1 - \dfrac{q}{s}\right)\tau_C & n = N_{\max} \end{cases} \tag{53}$$

$$w_{2n+2} = \begin{cases} (n+1)\tau_r + \tau_m + \dfrac{n_0+1}{s} & n = N_{\min} \\ n\tau_C + \tau_m + \tau_r - \dfrac{ns\tau_g - n_0 - 1}{q} & N_{\min} < n \le N_{\max} \end{cases} \tag{54}$$

Where k_j is the jam density which is the inverse of l and k_s is the capacity density.

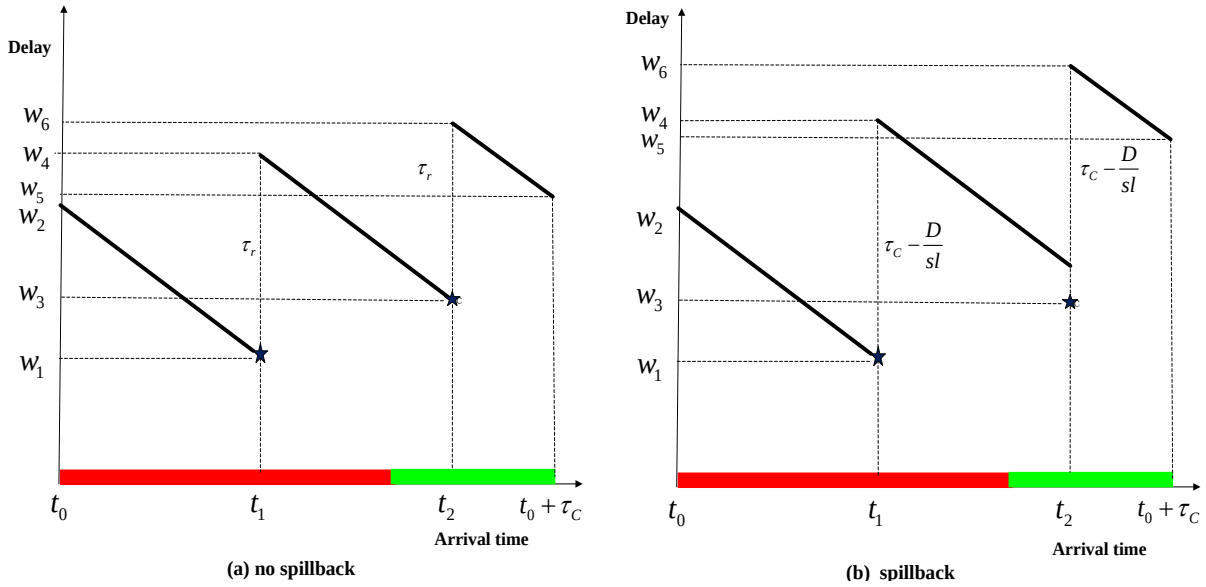

FIGURE 12 Delay as a function of arrival time for two intersections with pre-timed signal timings in the over-saturated condition

For an isolated intersection, the delay probability distribution in the undersaturated condition consists of a Dirac delta function and a box shaped function. While for the oversaturated condition, the probability distribution is the sum of some box shaped functions that may overlap. For the case of two adjacent intersections, once the delay at transition points is determined, by inverse mapping the delay to the arrival time and taking the derivative, the delay distribution can be derived similarly as shown in Figure 13. The probability distribution function for both the undersaturated and oversaturated condition is given by:

$$P_d(W\,|n_0) = \alpha(n_0)\delta(W) + \sum_N \beta B(W, W_{2N+1}(n_0), W_{2N+2}(n_0)) \tag{55}$$

Where α and β are model parameters with

$$\alpha = \max(\frac{s\tau_g' - n_0 - 1}{q\tau_C} - \frac{\tau_r + \frac{(n_0+1)}{s}}{\tau_C(1-\frac{q}{s})}, 0), \beta = \frac{1}{\tau_C(1-\frac{q}{s})},$$

W_{2N+1}, W_{2N+2} are delays at transition moments, which are given by Equations (39)- (42) and (51) - (54).

The general formulation of Equation (55) is very similar to Equation (4) of an isolated intersection. However, the parameter 'α' and the boundary delays 'W_{2N+1}, W_{2N+2}' in the box-shaped function are different from those of an isolated intersection.

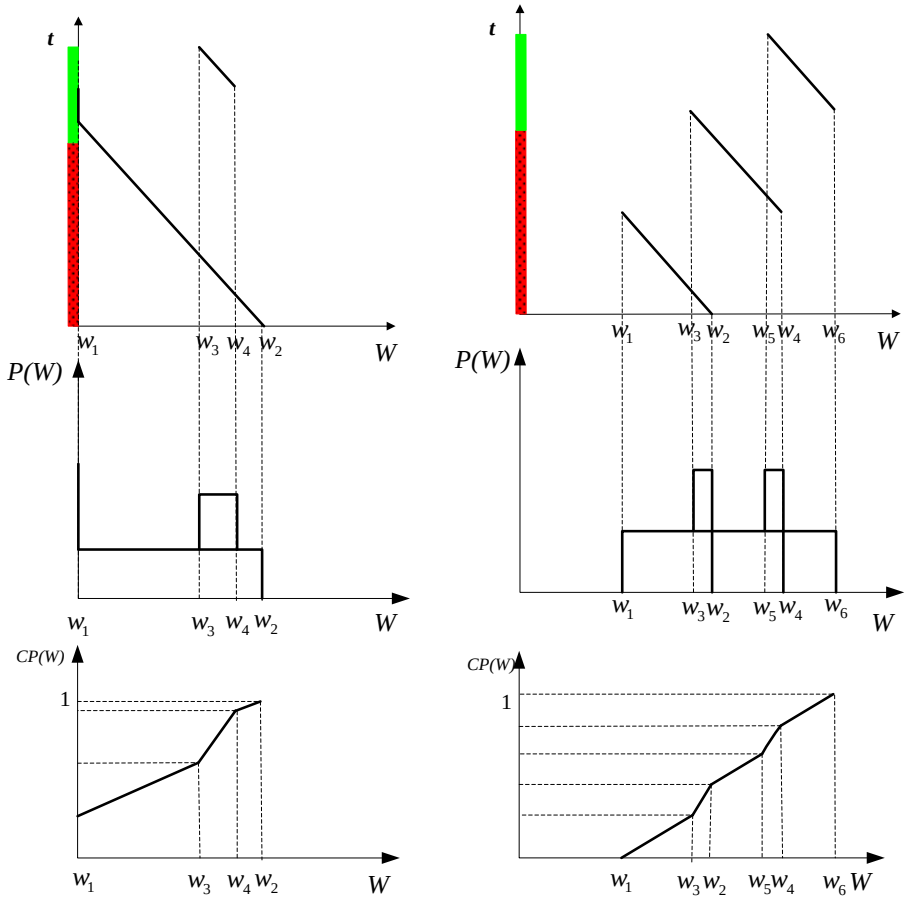

(a) Undersaturated condition (b) Oversaturated condition

Figure 13 Delay probability distribution and cumulative distribution for both undersaturated and oversaturated conditions

3.2.2 Delay distribution with a stochastic overflow queue

The delay probability distribution function derived in the previous subsection is based on the fixed initial queue that is present at the beginning of the green phase at the upstream (initial) intersection. If the initial queue is stochastic with a certain probability distribution, the expected probability distribution of the delay $P_d(W)$ can be calculated as a weighted sum of probability functions:

$$P_d(W) = \sum_{n_0=0}^{\infty} P_d(W \mid n_0) P(n_0) \tag{56}$$

where $P(n_0)$ is the probability of the overflow queue n_0.

3.3 Derivation of trip travel time distribution

In order to extend the model to trip travel time, first of all, the distribution of the 'free flow' travel time has to be determined. For an urban trip with two intersections or more, the delay is dependent on the free flow travel time. Fast drivers may encounter green waves along the trip while slow drivers may be stopped by the red light. The delay distributions for these two types of drivers are different. Furthermore, variable free flow travel time enables vehicles to take over each other. Therefore, for a given travel time τ ($\tau = w + \tau_f$), the probability of a certain delay w can be formulated as:

$$P_d\left(w \middle| \tau_f\right) = P_d\left(\tau - \tau_f \mid \tau_f\right) \tag{57}$$

Where $P_d(w \mid \tau_f)$ denotes the probability of a certain delay w given a certain free flow travel time τ_f with assumptions that vehicles cannot take over each other. $P_f(\tau_f)$ denotes the probability of a certain free flow travel time τ_f. If the variation of the free flow speed is very small such that vehicles cannot take over each other or in case of one single lane

traffic, the trip travel time distribution can be calculated by the following equation:

$$P(\tau) = \int_0^{\tau} P_d(\tau - \tau_f \mid \tau_f) P_f(\tau_f) d\tau_f \quad (58)$$

4. Results

4.1 Model validation with VISSIM simulation data

4.1.1 Single link travel time distribution

A single-lane link of 600m with one fixed time controlled intersection was modeled in VISSIM. Travel times for the complete link were recorded in VISSIM. The cycle time is 60s and effective green time is 24s. The number of simulation runs is 300 and the evaluation time for each simulation 1200s (20cycles). Two scenarios were chosen:

Scenario 1: The input flow is 720veh/h. The degree of saturation is about 0.833;

Scenario 2: The input flow is 807veh/h. The degree of saturation is about 0.917.

The free flow travel times were also recorded by letting vehicles travel through the link without interruption. The mean free flow travel time and the standard deviation were estimated based on the recorded data. A normal distribution was used as an approximation of the free flow travel time distribution in this study. Figure 14 compares the link travel time distributions derived from the proposed model and those from the VISSIM simulation model. The link travel time distributions derived from the analytical model can well represent those from the VISSIM simulation model for both scenarios. This can be confirmed by the Kolmogorov-Smirnov test (α=5%) results as shown in Figure . The hypothesis that simulated travel times come from the same distribution as the model predicted is not violated with the sample size of 500.

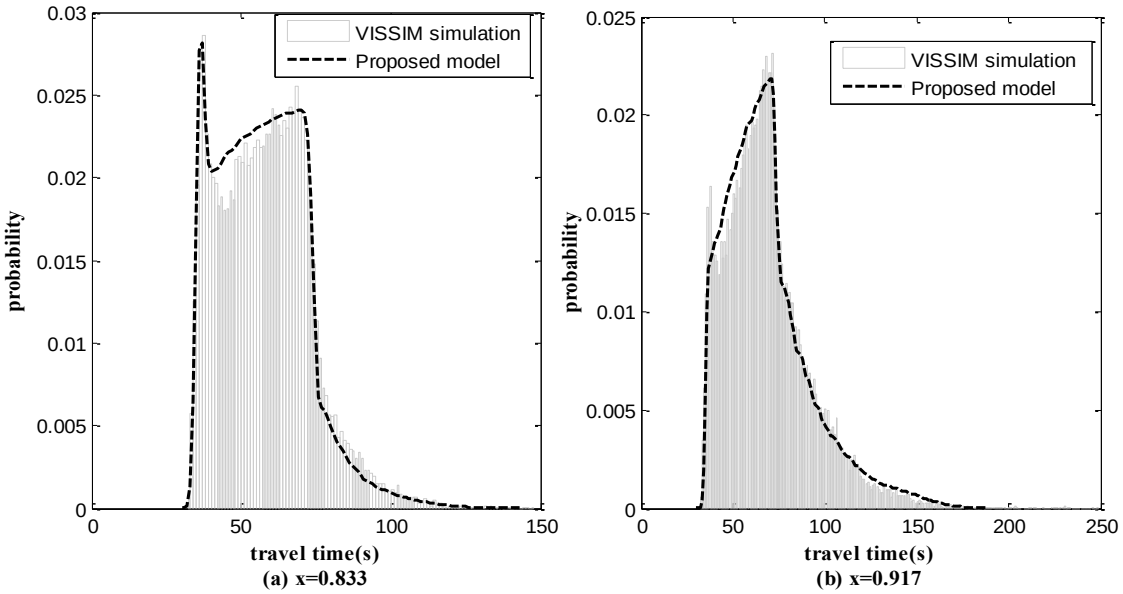

Figure 14 Comparison of the link travel time distribution between the analytical model and a VISSIM simulation model for a single intersection

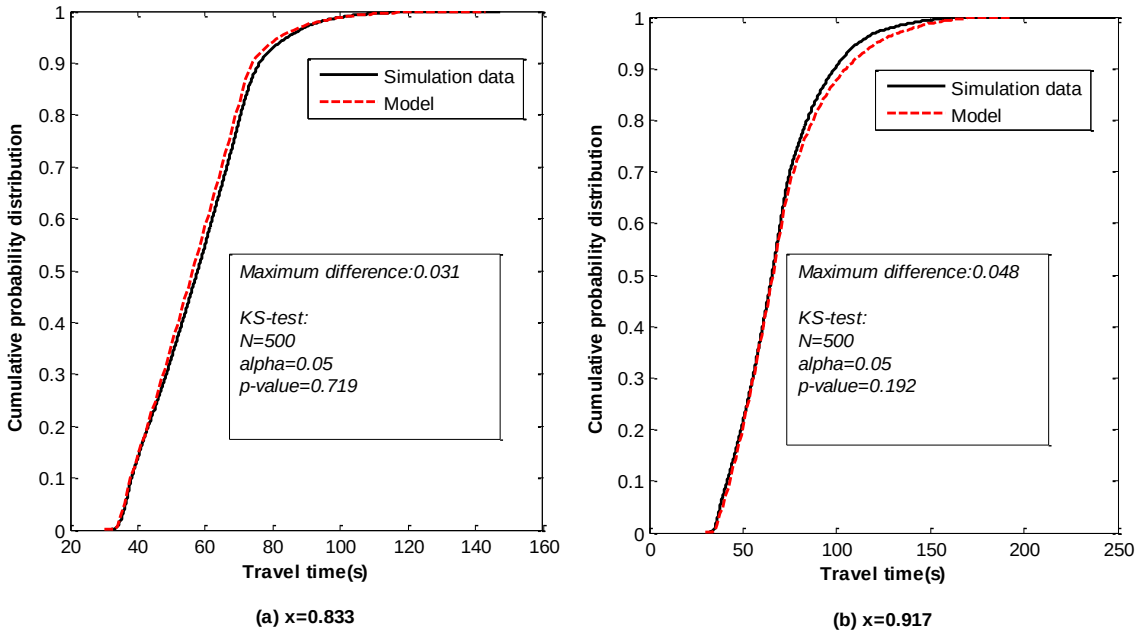

Figure 15 Kolmogorov-Smirnov test

4.1.2 Trip travel time distribution

1. Early green

An urban corridor composed of two fixed-time controlled intersections was built in VISSIM. The total length of the corridor is about 1200m and the desired speed is 60km/h.

The cycle time and effective green time for the through-going approach are the same for both intersections with 60s and 24s, respectively. The inflow is 800veh/h/lane. The simulation period is 1200s and a total of 300 realizations were simulated for each level of mismatch between two intersections (Four levels of mismatch: 0s, 5s, 15s and 20s). Travel times were recorded for each simulation run. Figure compares travel time distributions from the analytical model and those from the VISSIM simulation under the undersaturated condition (x =0.917). As can be seen from the figure, travel time distributions from the analytical model can well represent those from the simulation model under different levels of mismatch except that there is small discrepancy in low travel times and high travel times. This discrepancy could be the result of both the variable free flow travel time in VISSIM and stochastic arrivals and departures at the upstream intersection. Different free flow travel times modify vehicles' arrival moments at the downstream intersection. For instance, in case of early green mismatch, the first vehicle departing from the upstream intersection with smaller free flow travel time will arrive early and can decrease the influence of the mismatch for this vehicle. As a consequence, the vehicle experiences smaller delay compared with the delay estimated by assuming the average free flow travel time. The variation of inflow (stochastic arrivals) and outflow (stochastic departures) for each cycle at the upstream intersection influences the delay both at the upstream intersection and the downstream intersection. The discrepancy in the high travel times could be caused by the stochastic overflow queues due to stochastic arrivals and departures at the upstream intersection. Nevertheless, from the Kolmogorov-Smirnov test as illustrated in Figure , the hypothesis that the sample travel time

distribution generated in VISSIM and the travel time distribution from proposed model are drawn from the same distribution holds for different levels of mismatch.

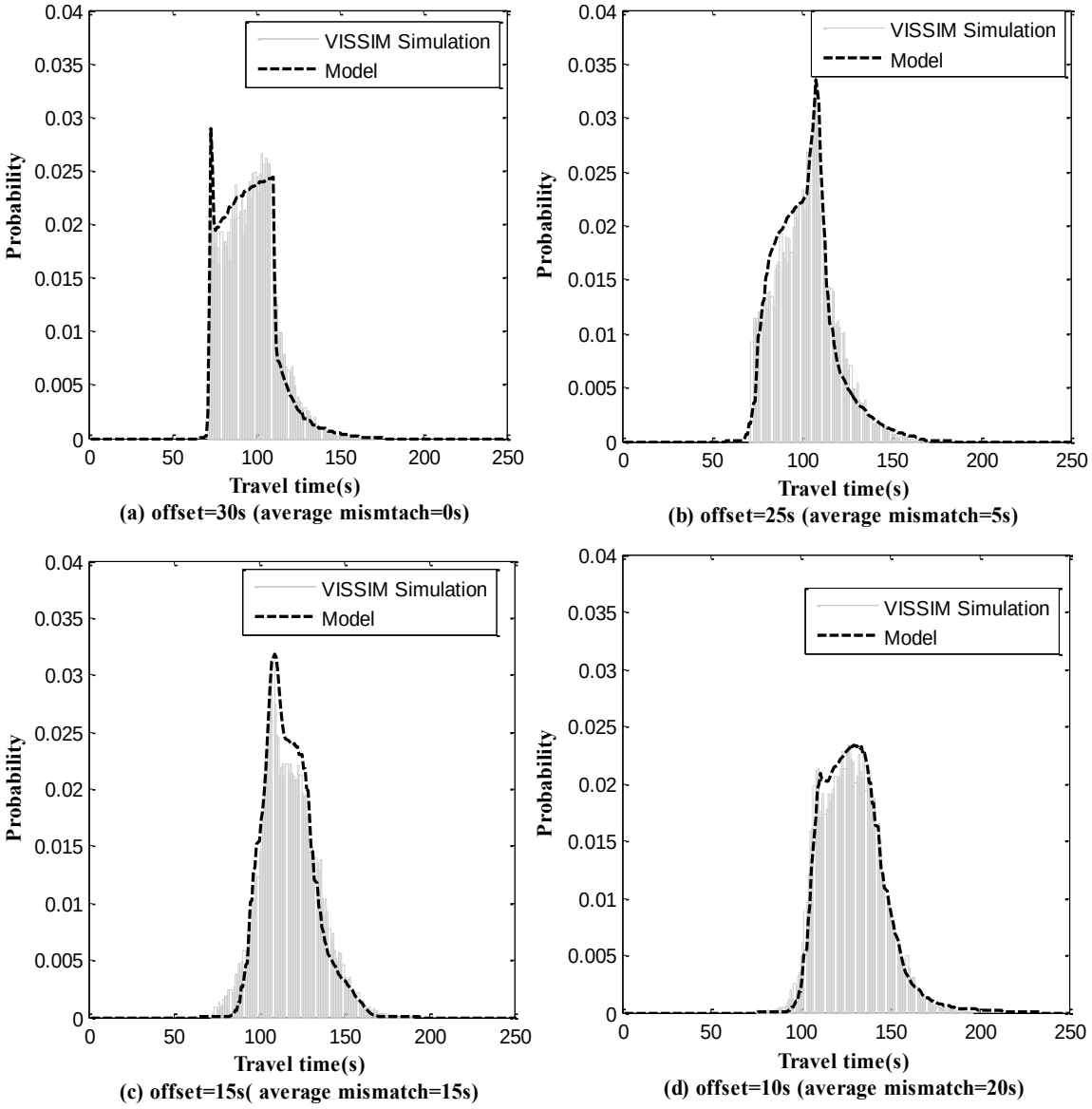

Figure 16 Trip travel time distributions for two signalized intersections and early green derived from the analytical model and a VISSIM simulation data with different level of mismatch 1 (q=800veh/h/lane, L=500m)

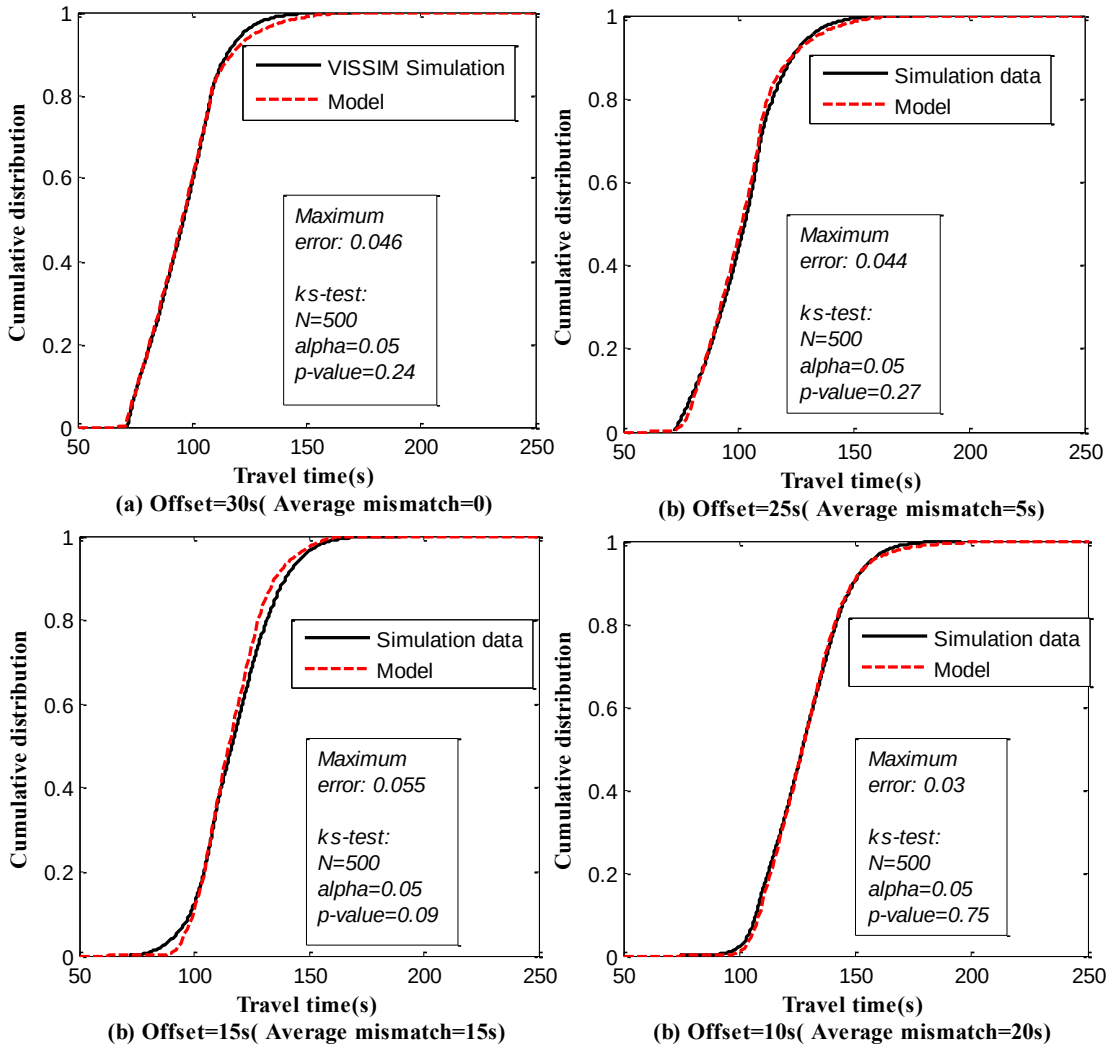

Figure 17 Kolmogorov-Smirnov test for different level of mismatch 1

2. Late green

In the case of late green, the total length of the corridor is about 1500m and the distance between two intersections is 100m. The distance between two intersections can be set to a different value as long as the spillback phenomenon occurs during the VISSIM simulation process. The average desired speed was set to be 60 km/h in VISSIM. The cycle time and effective green time for the through-going approaches are the same for both intersections with 60s and 24s, respectively. Table 1 indicates four cases investigated in this section and a total number of 300 realizations were simulated for each case. Both

for the under-saturated condition and the over-saturated condition, we chose different offsets to make sure that there is no spillback (offset = 10s) or spillback (offset = 25s) happening during the simulation process.

Table 1 Input data for VISSIM simulation in different traffic conditions

Traffic conditions	Traffic demand	Offset	Spillback
Under-saturated	700veh/h	10s	No
		25s	Yes
Over-saturated	1000veh/h	10s	No
		25s	Yes

In order to apply the proposed model to estimate travel time distributions, apart from signal control parameters some other parameters need to be determined, such as effective vehicle length in a queue, jam density, capacity density, expected saturation flow rate and free flow travel time, arrival and departure distributions. Table 2 indicates the values of these parameters in our model consistent with VISSIM with default parameters. The effective vehicle length was chosen such that it is consistent with that in VISSIM simulation model. The average saturation flow rate was determined by recording vehicles passing the intersection during the saturated green time in VISSIM. The arrival distribution at the upstream intersection is assumed to be Poisson distribution, and the departure distribution is Binomial distribution, both in VISSIM and in the analytic model. The free flow travel times were recorded by letting vehicles travel through the link without interruption. A normal distribution is able to represent the recorded free flow travel times quite well. Therefore, in our proposed analytical model, a normal distribution with the estimated mean value and the standard deviation was applied as an

approximation of the free flow travel time distribution in our proposed analytical model.

Table 2 Parameter values for the proposed model

Parameters	Effective vehicle length in the queue (m)	Jam density (veh/km)	Capacity density (veh/km)	Average saturation flow(veh/h)
Value	7	142	38	2250

Figure 18 compares travel time distributions from the proposed analytical model with those from the VISSIM simulation data in the under-saturated condition. The travel time distributions derived from the proposed model well represent those from the VISSIM simulation model both in the cases of no spillback (Figure 18 (a)) and spillback (Figure 18(b)). Figure 19 shows the comparison of travel time distributions in the over-saturated condition. It is clear that travel time distributions derived from the proposed analytical model represent those from VISSIM simulation rather well, though there are small discrepancies in low travel times and high travel times in the case of spillback.

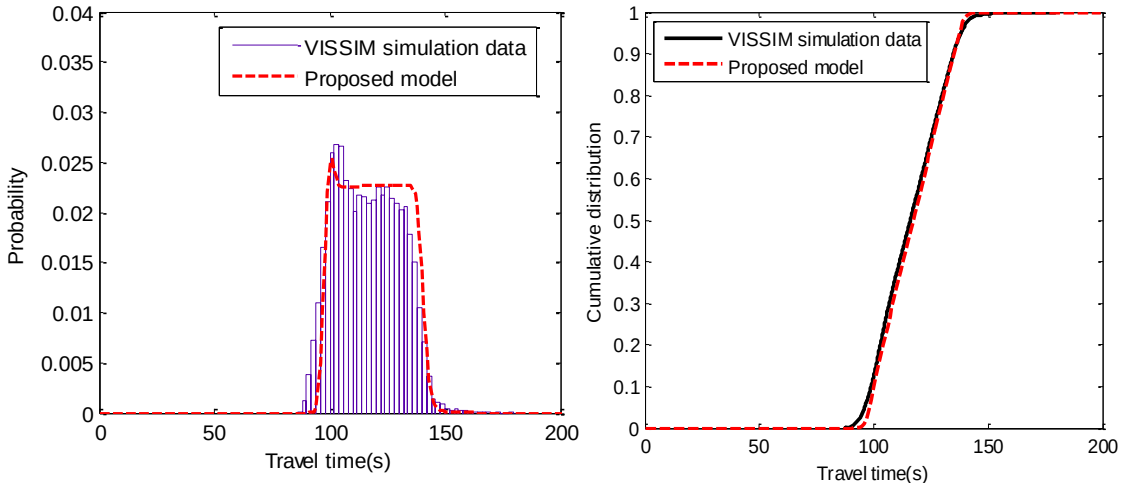

(a) no spillback (offset=10s)

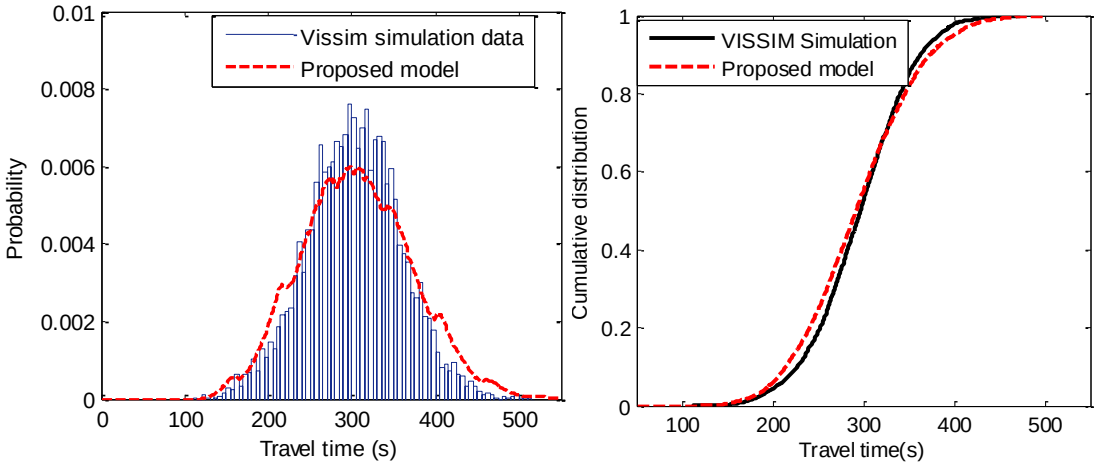

(b) With spillback (offset=25s)

Figure 18 Comparison of travel time distributions from VISSIM simulation data and the proposed model in the under-saturated condition (q=700veh/h/lane) with different offsets at 10th cycle

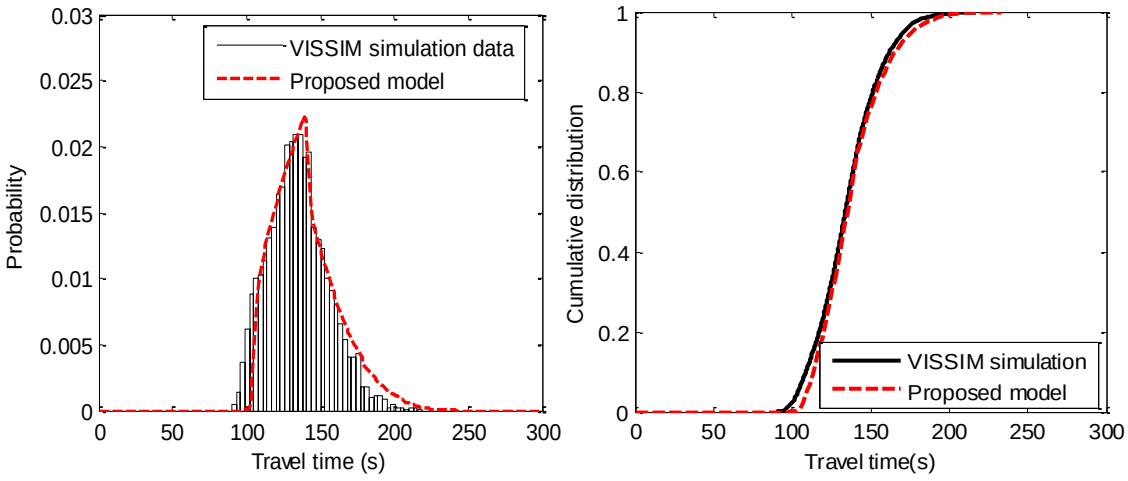

(a) no spillback (offset=10s)

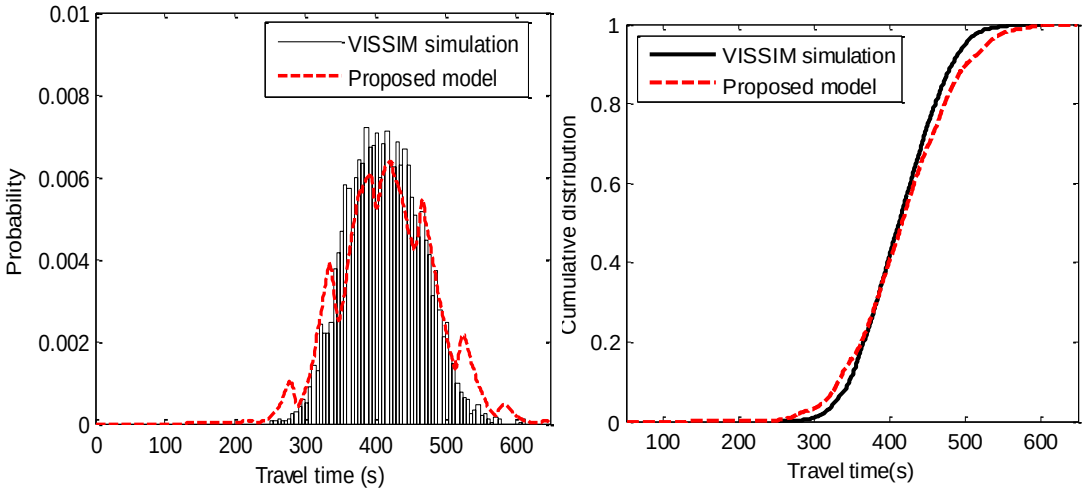

(b) With spillback (offset=25s)

Figure 19 Comparison of travel time distributions from VISSIM simulation data and the proposed model in the over-saturated condition (q=1000 veh/h/lane) with different offsets at 5th cycle

The spillback phenomenon can be observed frequently on urban roads with bad signal coordination, especially when two intersections are shortly distanced. If the spillback phenomenon is ignored during the modeling process, travel time distributions estimated from these models can be highly underestimated. As illustrated in Figure 20, we compared travel time distributions estimated from models considering spillback (the red dashed line) and without considering spillback (the blue dotted line) with the travel time distribution from VISSIM simulation (the black solid line). It is clear that when spillback is happening as simulated in VISSIM, the model ignoring the spillback phenomenon highly underestimates the travel time distribution. The reason behind is that if the existing spillback is not taken into account, the queue length at the downstream intersection will be highly underestimated, and the influence of spillback on the upstream intersection will be ignored. Therefore, it is necessary to take spillback into consideration when developing an analytical model for travel time distribution estimation.

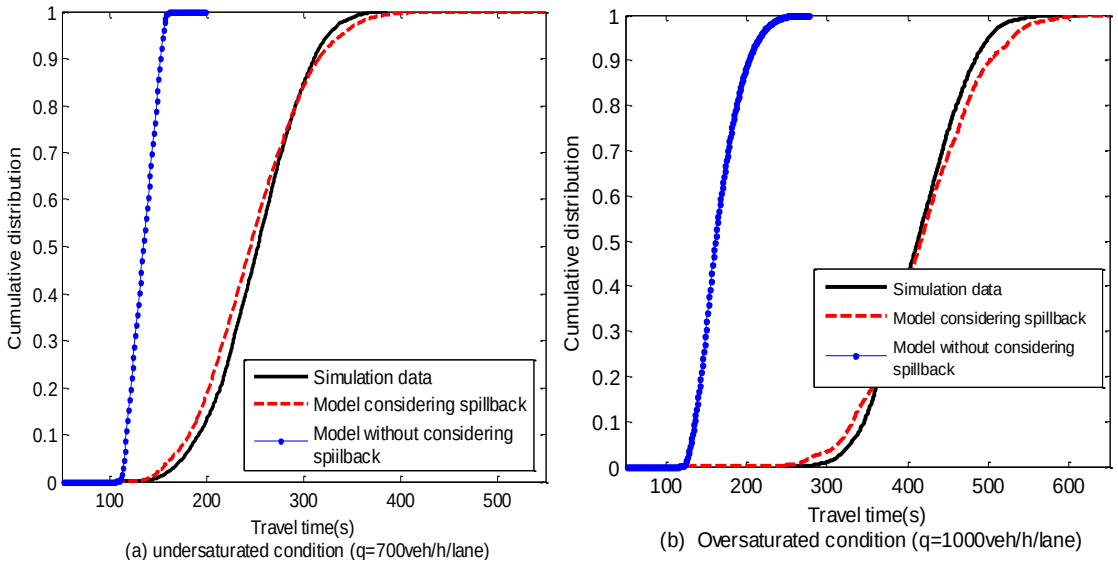

Figure 20 Comparison of travel time distributions (CDF) from VISSIM simulation and the proposed model considering and without considering spillback at 5th cycle

4.2 Comparison with field data

4.2.1 Test area

In the previous subsection, travel time distributions derived from the proposed model are compared with those from VISSIM simulation data. In this section, a test is performed with field data that were collected in Changsha, a Chinese city in Hunan Province. More than 6000 taxis equipped with GPS devices are used as probe vehicles travelling in the urban road network. Every 30s, positions, speeds and time stamps are recorded and sent to the monitoring center. Two links with signalized intersections indicated by arrows along Shaoshan Road were chosen as the test area shown in Figure .

Figure 21 The test road in Changsha city

4.2.2 Data and parameters

Travel times collected by GPS probe vehicles between 9:00AM and 10:AM on 14th, May 2010, and between 10:30 AM and 11:00AM on 15th, May 2010 are used for analysis and comparison. The GPS data were recorded every 30s which means that travel times recorded by probe vehicles provide only partial link or route travel times. In order to derive full link or route travel times, a method proposed by Li et al. (Li et al., 2010) is applied to reallocate travel times into individual links. Table indicates parameters of each link and intersection as well as the number of field travel time observations for each link. The average free flow speeds are estimated as the 50 percentile of the speeds from GPS data as measured on the middle of road sections. The saturation flow rate for each intersection was measured based on visual observations (Li et al., 2011). From the

analysis of the saturation flow for different lanes and intersections, the average saturation flow rates for through going lanes of intersections 11, 8, 3 are 1550veh/h/lane, 1560veh/h/lane and 1580veh/h/lane, respectively. The standard deviation among all these lanes is about 130veh/h. We assume that flows over these lanes of the same intersection are more or less the same. Table 4 indicates the parameters of route 13-11-8 during time period 9:00AM and 10:AM on 14th, May 2010.

Table 3 Parameters of links and intersections on 15th, May, 2010

Link	Link length(m)	Average infow(veh/h/lane)	Average free flow travel time(min)	Number of field travel time observations
13-11	1200	500	3	103
11-8	700	350	1.7	145
8-3	600	340	1.5	84

Intersection	Average cycle time(s)	Effective green time(s)	Saturation flow(veh/h/lane)
11	190	68	1550
8	190	53	1560
3	190	50	1580

Table 4 Parameters of route 13-11-8 on 14th, May

Time period	Average infow at the upstream intersection (veh/h/lane)	Average cycle time(s)	Effective green time(s)	Offset between intersection 11 and 8 (s)	Number of field travel time observations
9:00-9:30AM	450	220	70	183	33
9:30-10:00AM	470	212	65	180	34

4.2.3 Results

Figure illustrates the travel time distributions from GPS probe vehicle data and from the analytical model on link 13-11, link 11-8 and link 8-3 during period 10:30AM-11:00AM. Travel time distributions from the proposed model can represent the field travel time distributions reasonably well. However, middle range of travel times and higher

travel times are more frequently observed in field GPS data than the model predicts, especially for link 11-8. This discrepancy probably due to the fact that in the test road, there is a signalized pedestrian crossing which can cause extra delay to the through-going vehicles on link 11-8 as can be seen in Figure , while the proposed model does not consider the effect of turning movements from side streets between two signalized intersections. From the Kolmogorov-Smirnov test as shown in Figure (b) (d) (f), even with small GPS sample data, the hypothesis of a same distribution between the model and field data cannot be rejected. Figure 23 illustrates route travel time distributions derived from the model and from GPS probe vehicle data during periods 9:00 AM -9:30AM and 9:30 AM -10:00AM. Due to the fact that the number of travel times estimated from field GPS probe vehicle data is small (33 and 34 sample travel times during period 9:00AM-9:30AM and 9:30AM-10:00AM, respectively), the travel time distributions from GPS data are rather irregular. Some discrepancies between the model and GPS data can be observed, especially at the middle range of travel times. However, from the Kolmogorov-Smirnov tests shown in Figure 23 (b) and (d), the hypothesis of a same distribution between the proposed model and field GPS data cannot be rejected even with small sample size.

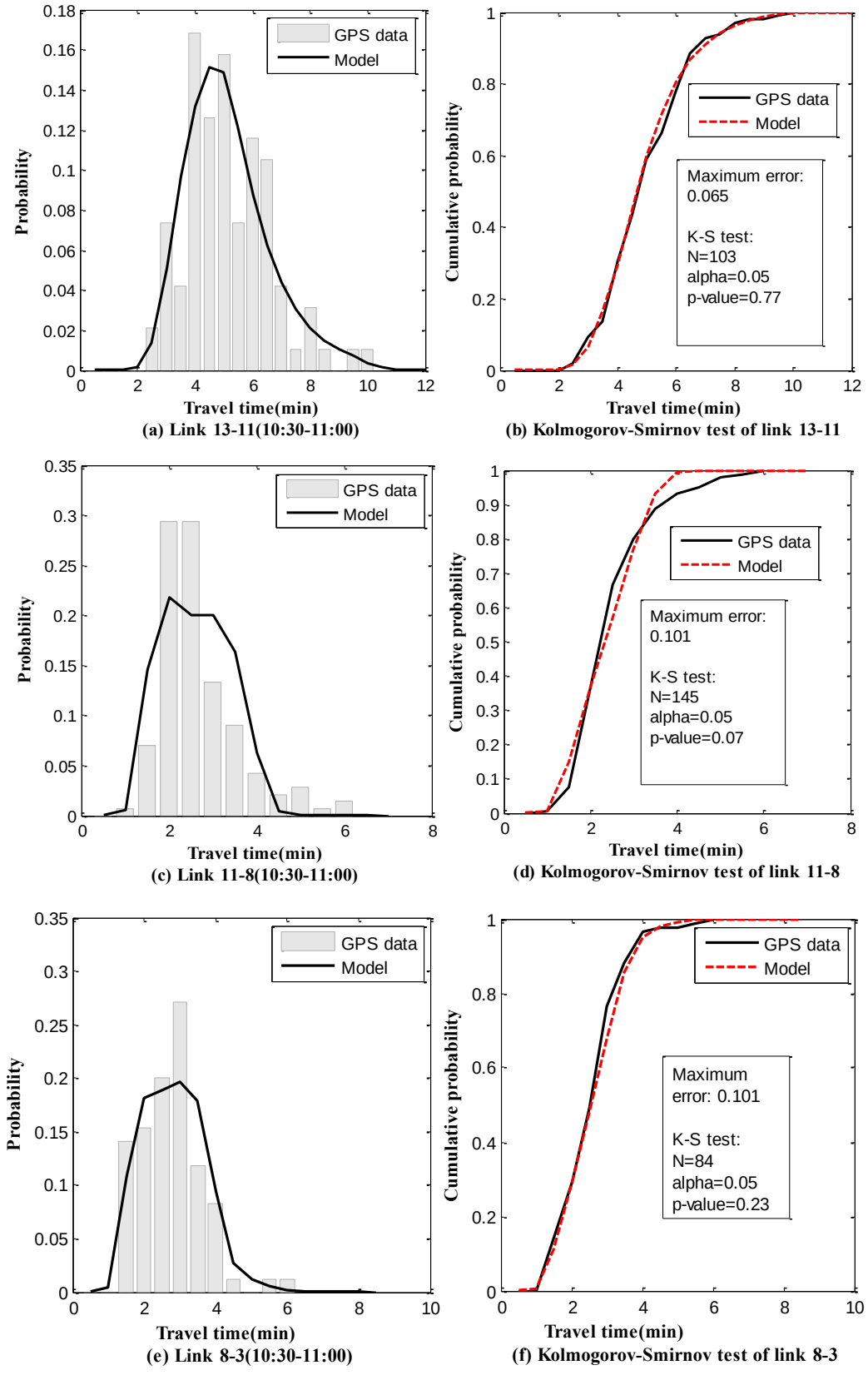

Figure 22 Comparison between travel time distributions from GPS probe vehicle data and those derived from the proposed model on link 13-11, link 11-8 and link 8-3, respectively (10:30 AM-11:00 AM)

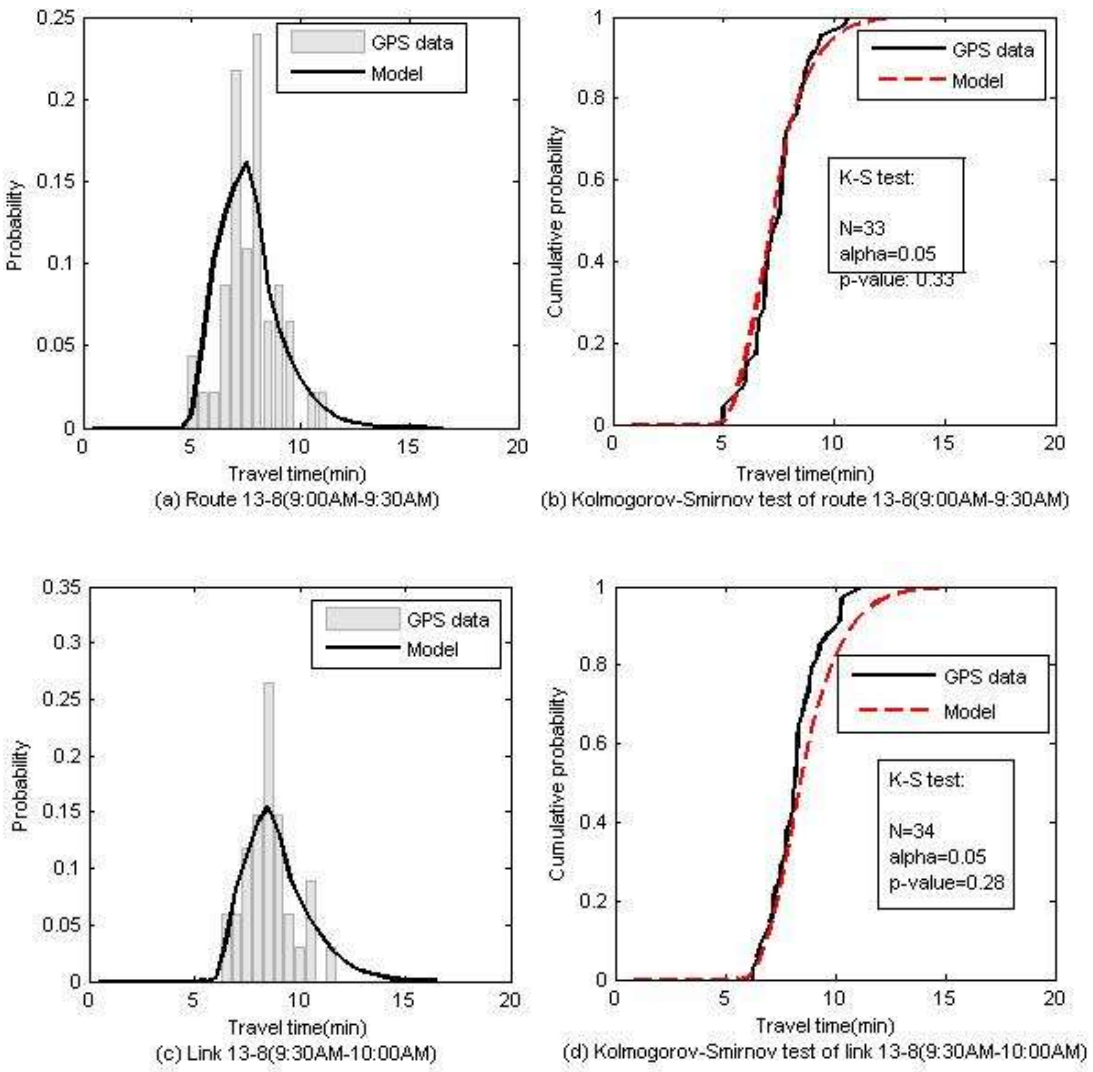

Figure 23 Comparison between travel time distributions from GPS probe vehicle data and those derived from the proposed model on route 13-11-8 during periods 9:00AM-9:30AM and 9:30AM-10:00AM, respectively

5. Possible extensions of the model

The objective of this study is to show how the travel time distribution on an urban route depends on certain controllable variables. The extension from a link with a single intersection to two links with two signalized intersections was made in the previous sections. In this extension, the basic mechanism is that the platoon travels from the upstream to the downstream intersection and that the stochasticity of the traffic flow is experienced at the inflow of the upstream intersection. This stochasticity of the traffic

arrivals is reflected in the initial queue at the start of the red phase on the upstream intersection (n_0).

This basic process can be extended to a longer route with three or more intersections. No fundamental new processes will occur, so that the travel time distribution for a route with three intersections can be derived from the two-intersection model extended with a deterministic platoon handling mechanism. A platoon handling model like the one in TRANSYT (Park and Schneeberger 2003) could calculate arrival patterns and travel time distributions for downstream links. An extension of the analytical method from two intersection routes to more intersections will create many possible situations to analyze: 2^{N+1} offset combinations and spill back conditions. Still each of these 2^{N+1} situations can be described by functions as derived in section 3.

The purpose of the analytical model is to reveal the influence of control parameters on the travel time distribution in order to be able to minimize travel time uncertainty. This can be done using the basic model with two intersections, possibly extended with a third road section with a third signalized intersection. Further extensions of the route will not give relevant new fundamental insights in the possibilities for the reduction of travel time variability.

Another, more important, extension of the analytical model is the inclusion of flows entering from the side. This can come from unsignalized intersections or entry/exit of a parking place. This will take away a part of the platoon flow and add a random flow. Since these uncontrolled flows have a random character, their influence on the queues of the second intersection will get a new stochastic character creating also a stochastic overflow

queue at the second intersection.

If the turning flow comes for the upstream signalized intersection, it will create a second platoon traveling to the downstream intersection. The extension of the model developed in section 3 will be that two consecutive platoons will arrive at the downstream intersection and the delay at the upstream intersection will be determined by two independent stochastic arrival processes. This extension of the model developed in section 3 is rather straight forwards and will be a subject for future further model development.

A final extension of the model is the inclusion of mid-link disturbances like bus stops and pedestrian crossing. This can be modeled in the probability distribution function of the free flow travel times such as in eq. (58). The detailed analysis of such phenomena is outside the scope of the present study.

6. Discussion and Conclusions

Urban travel time estimation is an important yet challenging topic. In recent years, focus of travel time estimation has been shifted from estimating expected travel times to estimating the variability of travel times, such as travel time distributions. With travel time probability distributions, the variability of travel times can be investigated straightforwardly using some statistical measures, e.g., standard deviation, percentiles, skewness, etc. In this paper, an analytical link travel time distribution model is proposed. The comparison of the results from the proposed model with those from the VISSIM simulation model shows that link travel time distributions based on the proposed model can well represent those from the simulation model. The comparison with field GPS data

indicates that model estimated link travel time distributions are not significantly different from field travel time distributions, though middle range and higher travel times are a little bit more frequently observed with GPS data than the model predicts for link 11-8 (Figure 22 (c)).

The extension of the link travel time distribution to the trip travel time distribution is also discussed. The model considers the stochastic properties of traffic flow, the signal coordination between intersections and takes the spillback into account as well. By considering the influence of stochastic arrivals and departures from the upstream intersection on the spillback from downstream intersection, the possibility of spillback is explicitly taken into consideration in the proposed model.

The comparison with VISSIM simulation shows that the travel time distributions estimated from the proposed model represents those from VISSIM simulation data well both in the under-saturated condition and the over-saturated condition with and without spillback. The comparison results also indicate that it is important to take the spillback phenomenon into account when developing travel time distribution models.

The model developed in this paper can be applied in different traffic conditions and further generalized to different traffic control schemes. The influence of traffic control schemes on the travel time distribution is explicitly modeled. The information of vehicle-to-vehicle travel time variations can help travelers to make better route choice. Besides, this model can be extended for travel time distribution prediction purpose.

Nevertheless, the model has some limitations: it considers a short corridor with pre-

timed traffic control. Furthermore the influence of turning movements on the intersections is ignored. The extension to corridor with 3 or more intersections and the inclusion of turning movements will result in more extended model with repetition of the elements of the model derived in this article.

In the future, we would like to investigate how to improve travel time reliability by optimizing traffic control schemes with this proposed model.

Acknowledgement

This research has been supported by the National Science Foundation of China (NSFC) under project 51308475, the Key Laboratory of Road and Traffic Engineering of the Ministry of Education, Tongji University under contract K20404 and Changsha Science and Technology Commission under project K1001010-11 and K1106004-11. The authors thank Li Jie from Hunan University for providing field traffic data in Changsha.

References

Bhaskar A., Chung E. &Dumont A. G.(2009) Travel time estimation on urban networks with mid-link sources and sinks. *In proceedings of TRB 88th Annual meeting.* Washington D.C.

Bhaskar A., Chung E. & Dumont A. (2011), Fusing loop detector and probe vehicle data to estimate travel time statistics on signalized urban networks, *Computer-Aided Civil and Infrastructure Engineering,* 26, 433–450.

Boel, R., Mihaylova, L., 2006. A compositional stochastic model for real time freeway traffic simulation. Transportation Research Part B 40, 319–334

Chen M. and Chien S.I.J. (2001) Dynamic freeway travel time prediction using probe vehicle data: Link-based vs. Path-based. *Transportation Research Record: Journal of the Transportation Research Board,* (1768):157-161

Chien S.I.J. and Kuchipudi C.M. (2002) Dynamic Travel Time Prediction with Real-time and Historical Data. *TRB 81st Annual meeting,* Washington D.C.

Cui X., Li Z. and Elefteriadou L. (2013). Travel time estimation for signalized arterials using probabilistic modeling *92nd TRB annual meeting*, Washington D.C..

Geroliminis N. & Skabardonis A. (2011), Identification and analysis of queue spillovers in city street networks, *IEEE Transactions on Intelligent Transportation Systems*, 12(4): 1107-1115.

Guo F., Rakha H. and Park S. (2010) A Multi-State Travel Time Reliability Model. *TRB 89th annual meeting*, Washington D.C.

Hofleitner A., Herring R., Abbeel P. & Bayen A. (2012), Learning the dynamics of arterial traffic from probe data using a dynamic Bayesian network, IEEE Transactions on Intelligent Transportation Systems, 13(4), 1679-1693.

Hurdle V.F. and Bongsoo S. (2001) Shock wave and cumulative arrival and departure models: partners without conflict. *Transportation Research Record: Journal of the Transportation Research Board*, 1776:159-166.

Innamaa S. (2005) Short-term prediction of travel time using neural networks on an interurban highway. *Transportation*, 32:649-669.

Kwon, J. and Petty K. (2005) A Travel Time Prediction Algorithm Scalable to Freeway Networks with Many Nodes with Arbitrary Travel Routes. *TRB 84th Annual Meeting*, Washington, D.C.

Li, M., Z. Zou and F. Bu (2010). Arterial Travel Time Estimation Using VII Probe Data and Point-based Detection Data. *13th International IEEE Annual Conference on Intelligent Transportation Systems*, Madeira Island, Portugal.

Li J., Zheng F., van Zuylen H.J. and Lu S.F. (2011). Calibration of a micro simulation program for a Chinese city. *Procedia Social and Behavioral Sciences*, 20 (2011):263–272.

Liu H. (2008) Travel time prediction for urban networks. PhD thesis, *TRAIL Thesis Series*, T2008/12.

Lo H.K. (2001) A cell-based traffic control formulation: strategies and benefits of dynamic timing plans. *Transportation Science*, 35(2):148-164.

Loustau Morency P., C. and Trepanier M. (2010) Measuring, describing and Modeling travel time reliability. T*RB 89th annual meeting*, Washington D.C.

Lu, Y. and Chang G.L. (2012). A Stochastic Model for Estimating the Time-Varying Arterial Travel Time and Its Variability Using Only Link Detector Data. *Transportation Research Board 91st Annual Meeting*, Washington D.C..

Olszewski P.S. (1994) Modeling probability distribution of delay at signalized intersections. *Journal of Advanced Transportation*, 28(3):253-274.

Osorio, C., Chong L. (2015) A computationally efficient simulation-based optimization algorithm for large-scale urban transportation problems. Transportation Science (to be published)

Park, B. and Schneeberger, J.D. Evaluation of traffic signal timing optimization methods using a stochastic and microscopic simulation program. *Virginia Transportation Research Council*, 2003.

Ramezani M. & Geroliminis N. (2012), On the estimation of arterial route travel time distribution with Markov chains, *Transportation Research Part B*, 46(10), 1576-1590.

Skabardonis A. and Geroliminis N. (2005) Real-time of travel times along signalized arterials. *Proceedings 16th International Symposium on Transportation and Traffic Theory*, University of Maryland, College Park, MD.

Skabardonis A. and Geroliminis N. (2008) Real-Time Monitoring and Control on Signalized Arterials. *Journal of Intelligent Transportation Systems: Technology, Planning, and Operations*, 12(2):64 - 74.

Sumalee, A., Zhong, R.X., Pan, T.L., Szeto, W.Y., 2011. Stochastic cell transmission model (SCTM): a stochastic dynamic traffic model for traffic state surveillance and assignment. Transportation Research Part B 45 (3), 507–533.

van Hinsbergen, van Lint C.P.I., J.W.C. and van Zuylen H.J. (2009) Bayesian training and committees of State Space Neural Networks for online travel time prediction. *Transportation Research Record: Journal of the Transportation Research Board*, (2105):118-126.

van Lint, J.W.C., Hoogendoorn S.P. and van Zuylen H.J. (2005) Accurate freeway travel time prediction with State-Space Neural Networks under missing data. *Transportation Research Part C:Emergency technologies*, 13(5-6):347-369.

van Zuylen H.J. and Hoogendoorn S.P. (2007). A Probabilistic calculation of queue lengths at signalized intersections. *ITS world congress*,Beijing.

Van Zuylen H.J., Viti F. (2006) Delay at controlled intersections: The old theory revised, IEEE Conference on Intelligent Transportation Systems, Proceedings, ITSC

Viti F. and Van Zuylen H.J. (2010) Probabilistic models for queues at traffic control signals. *Transportation Research Part B: Methodological*, 44(1):120-135.

Webster, F.V. (1958) Traffic signal settings, Road Research Laboratory, Her Majesty Stationary Offic e

Wu X. and Liu H. (2011). A shockwave profile mode for traffic flow on congested urban arterials. *Transport Research Part B: Methodological*, 45(2011):1768-1786.

Yun I, Park B (2006) Application of stochastic optimization method for an urban corridor. Proc. Winter Simulation Conf. (IEEE, Piscataway, NJ), 1493–1499

Yusuf I.T. (2010) The factors for free flow speed on urban arterials- Empirical evidences from Nigeria. *Journal of American Science*, 6(12):1487-1497.

Zheng F. and van Zuylen H.J. (2010). Uncertainty and Predictability of Urban Link Travel Time: A Delay Distribution Based Analysis. *Transportation Research Record: Journal of the Transportation Research Board*, 2192:136-146.

Zheng F. and van Zuylen H.J. (2014). The development and calibration of an urban travel time distribution model. *Journal of Intelligent Transportation Systems: Technology, Planning and Operations*, 2014, 18(1): 81-94.

Zheng F. and van Zuylen H.J. (2013). Trip travel time distribution prediction for urban signalized arterials. Presented in *International Conference on Transportation Engineering, Chengdu*, P.R.China .

Zheng F., van Zuylen H.J., Zhang J. and Jin L (2015). Travel time distribution estimation for urban signalized arterials considering spillback. Presented in *94th TRB annual meeting*, Washington D.C., U.S.